

Central Exclusive χ_c Meson Production at the Tevatron Revisited

L.A. Harland-Lang¹, V.A. Khoze^{2,3}, M.G. Ryskin^{2,4}, W.J. Stirling^{1,2}

¹ *Cavendish Laboratory, University of Cambridge, J.J. Thomson Avenue, Cambridge, CB3 0HE, UK*

² *Department of Physics and Institute for Particle Physics Phenomenology, University of Durham, DH1 3LE, UK*

³ *School of Physics & Astronomy, University of Manchester, Manchester M13 9PL, UK*

⁴ *Petersburg Nuclear Physics Institute, Gatchina, St. Petersburg, 188300, Russia*

ABSTRACT: Motivated by the recent experimental observation of exclusive χ_c events at the Tevatron, we revisit earlier studies of central exclusive scalar χ_{c0} meson production, before generalising the existing formalism to include χ_{c1} and χ_{c2} mesons. Although χ_{c0} production was previously assumed to be dominant, we find that the χ_{c1} and χ_{c2} rates for the experimentally considered $\chi_c \rightarrow J/\psi\gamma \rightarrow \mu^+\mu^-\gamma$ decay process are in fact comparable to the χ_{c0} rate. We have developed a new Monte Carlo event generator, SuperCHIC, which models the central exclusive production of the three χ_c states via this decay chain, and have explored possible ways of distinguishing them, given that their mass differences are not resolvable within the current experimental set-up. Although we find that the severity of current experimental cuts appears to preclude this, the acceptance does not change crucially between the three states and so our conclusions regarding the overall rates remain unchanged. This therefore raises the interesting possibility that exclusive χ_{c1} and χ_{c2} production has already been observed at the Tevatron.

1. Introduction

The measurement of central exclusive production (CEP) processes in high-energy proton – (anti)proton collisions represents a very promising way to study the properties of new particles, from exotic hadrons to the Higgs boson, see for example Refs. [1] – [7].

The CEP of an object A may be written in the form

$$pp(\bar{p}) \rightarrow p + A + p(\bar{p}),$$

where $+$ signs are used to denote the presence of large rapidity gaps. An attractive advantage of these reactions is that they provide an especially clean environment in which to measure the nature and quantum numbers (in particular, the spin and parity) of new states, see for example Refs. [4, 8, 9]. A topical example is the CEP of the Higgs boson [10] – [14]. This provides a novel and promising way to study in detail the Higgs sector at the LHC and gives a strong motivation for the addition of near-beam proton detectors to enhance the discovery and physics potential of the ATLAS and CMS detectors at the LHC [15] – [17].

Recently, exclusive diffractive processes $p\bar{p} \rightarrow p + A + \bar{p}$ have been successfully observed by CDF Collaboration at the Tevatron, where $A = \gamma\gamma$ [18], dijet [19] or χ_c [20].¹ As the sketch in Fig. 1(a) indicates, these processes are driven by the same mechanism as exclusive Higgs (or other new object) production at the LHC, but have much larger cross sections. They can therefore serve as “standard candles”, see [12, 23], which allow us to check the theoretical predictions for the CEP of new physics signals by measurements made at the Tevatron. Moreover, the observed rates of all three CEP processes measured by the CDF collaboration are in broad agreement with theoretical expectations [3, 5, 12, 23], which lends credence to the predictions for exclusive Higgs production at the LHC.

Among the CEP processes measured at the Tevatron, the double-diffractive production of C-even, heavy quarkonia (χ_c) states plays a special role [5] (see also [24] – [29]). First, as is well known, heavy quarkonium production provides a valuable tool to test the ideas and methods of the QCD physics of bound states, such as effective field theories, lattice QCD, NRQCD, etc. (see, for example, Refs. [30, 31] for theoretical reviews). Second, χ_c production exhibits characteristic features, based on Regge theory, that depend on the particle spin and parity J^P . We discuss these in Section 2 below.

A potential problem with χ_c production as a “standard candle” for Higgs production is that it is far from clear that the purely perturbative approach of Refs. [10, 12] (as exemplified by Fig. 1(a)) is valid. In particular, the estimates in Ref. [5] assume a perturbative contribution coming from integrating round the gluon loop in Fig. 1(a) for $Q_\perp > 0.85$ GeV. Due to such low scales, strictly speaking one cannot guarantee that the accuracy in the perturbative predictions made in this way for χ_c CEP is better than a factor of 4-5 up or down. In addition, there may be important non-perturbative contributions, traditionally modelled by the Pomeron-Pomeron process shown in Fig. 1(b), but

¹For a recent review see [21]. More CDF exclusive data on $\gamma\gamma$ and χ_c production may be available in the near future [22].

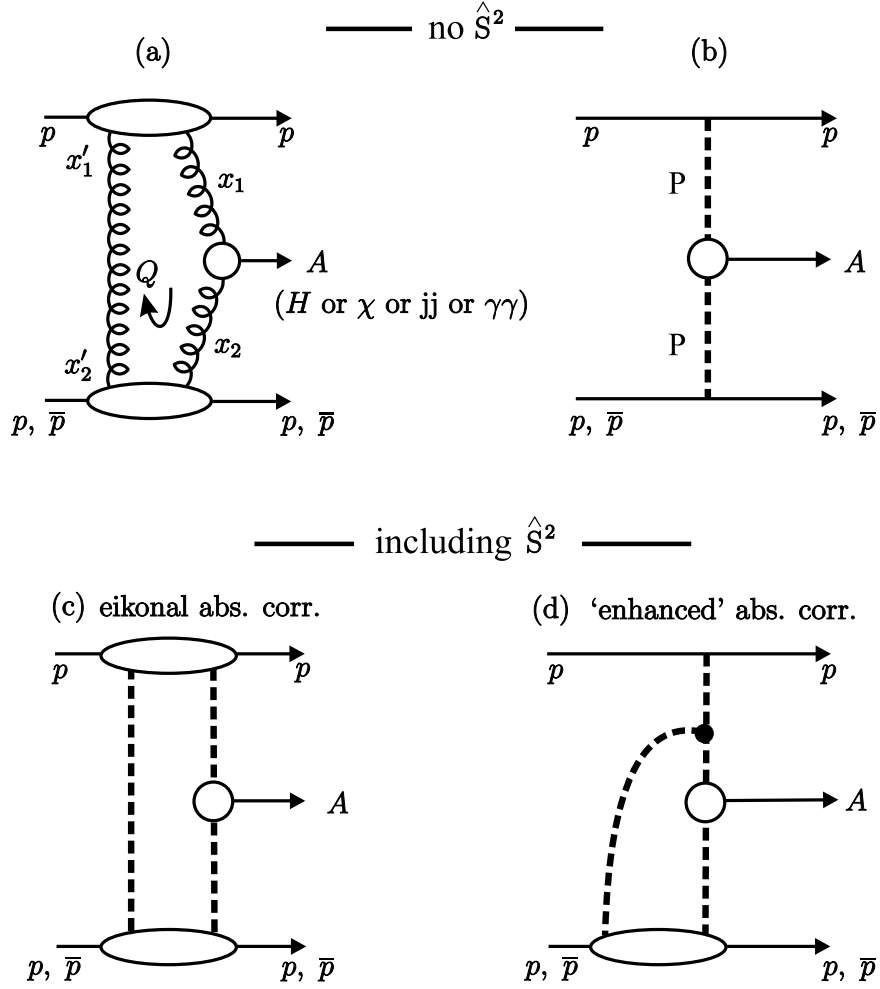


Figure 1: Schematic diagrams for CEP of a system A within the approach of Refs. [10, 12] and [32] - [35]. The integration over the loop momentum Q_\perp in diagram (a) results in a $J_z = 0$ selection rule [3], where J_z is the projection of the total angular momentum along the proton beam axis. It is also necessary to compute the probability, \hat{S}^2 , that the rapidity gaps survive soft ([32, 33]) and semi-hard ([34] - [36]) rescattering; these two possible types of unitarity (or absorptive) corrections are exemplified in diagrams (c) and (d) respectively, where the dashed lines represent Pomeron exchanges (as in version (b) of diagram (a)).

here again there is significant model dependence and so any predictions for this component also come with large uncertainties. We choose to take a pragmatic approach, in which we base our analysis on the perturbative contribution only, but at the same time we consider which features of the perturbative contribution (for example, the relative contributions of the various J^P states, distributions of final state particles, etc.) are likely to be shared by the non-perturbative contribution. Independent of the exact details of the production mechanism, the CEP of χ states provides a valuable check on the important ingredients of the physics of Pomeron-Pomeron fusion.

Another important issue related to the CEP of χ_c states at the Tevatron is that this

process allows us to test the role of the so-called enhanced absorptive corrections (see Fig. 1(d)), which break soft-hard factorization, see for example [35] - [36]. As shown in [14, 35], there is a hierarchy in the value of the rapidity gap survival factor S due to enhanced absorption, S_{enh} ,

$$S_{\text{enh}}^{\text{LHC}}(M_H > 100 \text{ GeV}) > S_{\text{enh}}^{\text{Tevatron}}(\gamma\gamma; E_T^\gamma > 5 \text{ GeV}) > S_{\text{enh}}^{\text{Tevatron}}(\chi_c),$$

which reflects the size of the various rapidity gaps (s/M^2) of the different exclusive processes. The very fact that $\gamma\gamma$ and χ_c events have been observed at the Tevatron in reasonable agreement with theoretical expectations² confirms that there is no danger that enhanced absorption will strongly reduce the exclusive SM Higgs signal at the LHC.

When interpreting the results of [20] in terms of the production of a particular χ_c state there is one important point to bear in mind. While the P and C parities are unambiguously defined by the fusion mechanism (see, for example, [12]) the spin assignment requires special care. As discussed in Refs. [3, 5], central exclusive χ_c production should be dominated by the $\chi_{c0}(0^{++})$ state. This is because $\chi_{c1}(1^{++})$ and $\chi_{c2}(2^{++})$ production is *strongly suppressed*: the former due to the Landau-Yang theorem [38] for on-mass-shell gluons and the latter because in the non-relativistic approximation the $\chi_{c2}(2^{++})$ meson cannot be produced in the $J_z = 0$ state, which dominates CEP for forward outgoing protons [3].

Recall, however, that the experimental observation [20] of exclusive χ_c production is based on the decay chain $\chi_c \rightarrow J/\psi\gamma \rightarrow \mu^+\mu^-\gamma$. The observed 65 ± 10 signal events have a limited $M(J/\psi\gamma)$ resolution and are collected in a restricted area of final state kinematics (due to cuts and event selection criteria). In order to determine the χ_c yield the dominance of χ_{c0} production is *assumed*, and the CHIC Monte Carlo³, based on the $\chi_{c0} \rightarrow J/\psi + \gamma$ decay, is used for conversion of the observed events into the cross section. However at the present time we cannot rule out the possibility that, under the conditions of the CDF experiment, higher spin χ_c states (1^{++} , 2^{++}) contribute to the observed $J/\psi + \gamma$ signal.⁴ As is correctly pointed out in Ref. [29], the strong suppression of 1^{++} central production can be compensated by its much higher branching fraction to the $J/\psi + \gamma$ final state. We show below (see also [14]) that this can also be true for $\chi_{c2}(2^{++})$ CEP. Explicitly, the χ_{c0} , χ_{c1} , χ_{c2} branching fractions to $J/\psi\gamma$ are 0.011, 0.34 and 0.19 respectively [37]. There is another factor leading to a further rebalance between the relative contributions of different χ_c spin states. As discussed in [4, 14], the eikonal survival factor, S_{eik} , is larger for χ_{c1} and χ_{c2} since, due to their spin structure, they are produced more peripherally.⁵

The simultaneous presence of several χ_c states clearly requires a more comprehensive analysis, including a new Monte Carlo programme, allowing for production and decay of

²In the χ_c case the agreement becomes especially striking after taking into account the revised value of the total χ_{c0} width which has been reduced by a factor 1.4 [37] as compared to the value in the Review of Particle Properties (2002) used in [5].

³CHIC is a publicly available Monte Carlo implementation of the χ_{c0} analysis of Ref. [5].

⁴This applies not only to $\chi_c(1P)$ states, but also to possible higher excitations $\chi_c(nP)$.

⁵ S_{enh} is largely independent of the χ spin assignment. Note also that the relative number of events where the forward protons dissociate is larger for χ_{c1} and χ_{c2} than for χ_{c0} .

the higher-spin states. This is the main topic of the current paper, i.e. we extend the analysis of Refs. [3, 5] to include the detailed study of χ_{c1} and χ_{c2} exclusive production. Special attention is paid to the role of absorptive corrections, which significantly affect the predicted rates, see [4, 5, 14].

The paper is organized as follows. In Section 2 we review the general expectations for the J^P properties of χ_c production based on Regge theory. In Section 3 we discuss in detail the perturbative approach to the calculation of χ_c CEP, paying particular attention to the differences between χ_{c0} , χ_{c1} and χ_{c2} production and to the uncertainties in the predictions. We have implemented our calculations in a new Monte Carlo event generator – SuperCHIC – which is described in Section 4. In Section 5 we present numerical results for χ_{c0} , χ_{c1} and χ_{c2} CEP at the Tevatron. We discuss the impact of the survival factors on the CEP cross sections, and comment on the size of possible non-perturbative contributions. We investigate to what extent kinematical distributions of the final-state particles can be used to distinguish the three χ_c spin states. In Section 6 we summarise our conclusions and comment on possible future developments in the study of the CEP of quarkonia states at the Tevatron and LHC. Some additional calculational details are presented in two Appendices.

2. General expectations from Regge theory

As discussed in [4], the central diffractive production of meson states (see Fig. 1(b)) has characteristic features that depend on the particle spin and parity J^P , which follow from the general principles of Regge theory. Let us first recall particular examples of *bare* Pomeron-Pomeron vertices for the spin-parity J^P of particle h in the case of low transverse momenta $\mathbf{p}_{1,2\perp}$ of the outgoing protons.

(a) $J^P(h) = 0^+$

For a scalar particle h , the vertex coupling is simply⁶

$$g_{PP}^S = f_{0+}(\mathbf{p}_{1\perp}^2, \mathbf{p}_{2\perp}^2, \mathbf{p}_{1\perp} \cdot \mathbf{p}_{2\perp}), \quad (2.1)$$

where f_{0+} is a function of the displayed scalar variables. When $\mathbf{p}_{1\perp}^2$ or $\mathbf{p}_{2\perp}^2 \rightarrow 0$, this function, in general, tends to some constant f_s . Further information on the structure of this function requires extra dynamical input. In particular, within the perturbative framework (for $\mathbf{Q}_\perp^2 \gg \mathbf{p}_{1,2\perp}^2$), f_{0+} is almost independent of $\mathbf{p}_{1,2\perp}$, and hence the bare cross section, σ_{0+} , is essentially independent of the azimuthal angle ϕ between the outgoing protons

$$\frac{d\sigma_{0+}}{dt_1 dt_2 d\phi} \propto \text{constant}(\phi), \quad (2.2)$$

where $t_{1,2} \simeq -\mathbf{p}_{1,2\perp}^2$. We note, however, that for χ_c CEP the low Q_\perp scale we are considering means that the inequality $\mathbf{Q}_\perp^2 \gg \mathbf{p}_{1,2\perp}^2$ is not completely valid, and we therefore expect some deviation from the constant behaviour of (2.2).

⁶We use boldface type to denote spatial three-vectors.

(b) $J^P(h) = 0^-$

For the central production of a pseudoscalar particle, the bare vertex factor takes the form

$$g_{PP}^P = f_{0-}(\mathbf{p}_{1\perp}^2, \mathbf{p}_{2\perp}^2, \mathbf{p}_{1\perp} \cdot \mathbf{p}_{2\perp}) (\mathbf{p}_{1\perp} \times \mathbf{p}_{2\perp}) \cdot \mathbf{n}, \quad (2.3)$$

where \mathbf{n} is the unit vector in the direction of the colliding hadrons (in the c.m.s.). Due to the identity of the Pomerons, the function f_{0-} should be symmetric under the interchange $1 \leftrightarrow 2$. It follows from (2.3) that in the pseudoscalar case the bare cross section, σ_{0-} , should behave for small $|t_{1,2}|$ as

$$\frac{d\sigma_{0-}}{dt_1 dt_2 d\phi} \propto |t_1| |t_2| \sin^2 \phi. \quad (2.4)$$

An immediate consequence of (2.4) is that pseudoscalar production is forbidden when the protons scatter at zero angle.

(c) $J^P(h) = 1^+$

For the production of an axial vector state the bare Pomeron-Pomeron fusion vertex factor can be written as

$$g_{PP}^A \sim a_{\lambda=0} \frac{(t_1 - t_2)([\mathbf{p}_{1\perp} \times \mathbf{p}_{2\perp}] \cdot \mathbf{e})}{M^2} + a_{\lambda=1} \frac{[\mathbf{K} \times \mathbf{n}] \cdot \mathbf{e}}{M} \quad (2.5)$$

with

$$\mathbf{K} \equiv \mathbf{p}_1 - \mathbf{p}_2. \quad (2.6)$$

Here M and \mathbf{e} are the mass and polarization vector of the centrally produced 1^{++} state, and the vertex functions $a_{\lambda=0,1}$ correspond to axial meson production with helicities $\lambda = 0, 1$ in the target rest frame (where the longitudinal component of the axial meson momentum is much larger than its transverse component). Analogously to f_{0+} and f_{0-} in the previous cases, the functions $a_{\lambda=0,1}$ may depend on $\mathbf{p}_{1\perp}^2$, $\mathbf{p}_{2\perp}^2$ and $(\mathbf{p}_{1\perp} \cdot \mathbf{p}_{2\perp})$, and are symmetric under the $1 \leftrightarrow 2$ interchange.

It follows from (2.5) that the bare amplitude tends to zero at low K_\perp , in particular when both protons scatter at zero angle. Another important consequence of (2.5) is that at low $|t_{1,2}|$ the axial meson should be produced dominantly in the helicity-one state. As already mentioned in [4], the general structure of the axial vertex g_{PP}^A , given by Eq. (2.5), coincides with that found using a non-conserved vector current model [8], which gives a good description of the experimental data on $f_1(1285)$ and $f_1(1420)$ CEP by the WA102 Collaboration [39]; for a review see Ref. [7].

(d) $J^P(h) = 2^+$

For a tensor particle h , the bare vertex function g_{PP}^T is not constrained by Regge theory alone. However, as we have already mentioned, within the perturbative approach of Refs. [5, 12] the forward CEP of non-relativistic heavy 2^{++} quarkonium

should be strongly reduced because of the suppression of the $2^{++} \rightarrow 2g$ transition for the $J_z = 0$ on-mass-shell two-gluon state.⁷

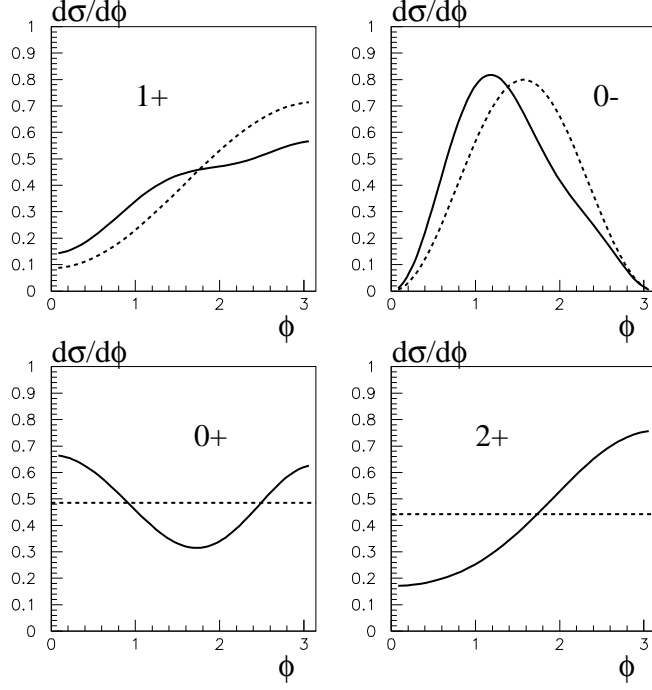


Figure 2: Impact of the absorptive corrections on the distribution (in arbitrary units) of the difference in azimuthal angle of the outgoing protons for the CEP of various J^P χ_c states at the LHC, using the two channel eikonal model of Ref. [32]. The solid (dashed) lines are the distributions including (excluding) the survival factor. For completeness we also show the result for pseudoscalar η_c production.

Finally, we recall that, as discussed in [4], the absorptive corrections arising from the multi-Pomeron exchanges modify the distributions over ϕ . This is because the absorption depends on the distribution in impact parameter \mathbf{b} space, which in turn leads to a characteristic dependence of the survival factor (mainly S_{eik}^2) on the azimuthal angle between the outgoing protons. This effect was discussed in detail in [40].

To demonstrate how the absorptive corrections may affect the angular distributions between the outgoing protons we have used a simple two channel eikonal model [32]. We show in Fig. 2 the results for $\sqrt{s} = 14$ TeV. An analogous dependence of S_{eik}^2 on the transverse momentum of the centrally produced meson is shown for the Tevatron energy $\sqrt{s} = 1.96$ TeV in Fig. 3.

⁷We reconfirm the conclusion of [3] that the relativistic corrections to the $\chi_{c,b}(2^{++}) \rightarrow 2g$ transition are numerically small.

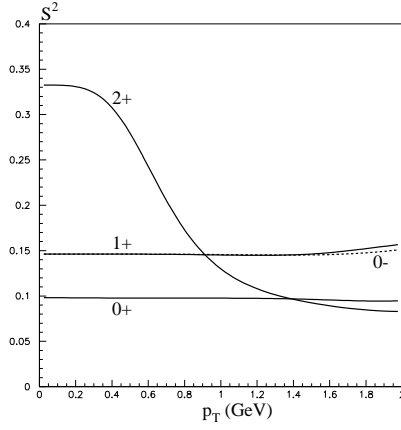


Figure 3: Dependence of the survival factor S_{eik}^2 on the transverse momentum of centrally produced χ_c mesons at the Tevatron, using the two channel eikonal model of Ref. [32]. Also shown (dashed line) is the survival factor corresponding to η_c production.

3. Central Exclusive χ_c production: perturbative framework

To calculate the perturbative contribution to the central exclusive χ_c production process we use the formalism of Refs. [3, 4, 10]. The amplitude is described by the diagram shown in Fig. 1(a), where the hard subprocess $gg \rightarrow \chi_c$ is initiated by gluon-gluon fusion and the second t -channel gluon is needed to screen the colour flow across the rapidity gap intervals. We can write the Born amplitude in the factorised form [5, 6] (see Fig. 4):

$$T = \pi^2 \int \frac{d^2 \mathbf{Q}_\perp V_J}{\mathbf{Q}_\perp^2 (\mathbf{Q}_\perp - \mathbf{p}_{1\perp})^2 (\mathbf{Q}_\perp + \mathbf{p}_{2\perp})^2} \cdot f_g(x_1, x'_1, Q_1^2, \mu^2; t_1) f_g(x_2, x'_2, Q_2^2, \mu^2; t_2) , \quad (3.1)$$

where V_J is the colour-averaged, normalised sub-amplitude for the $gg \rightarrow \chi_{cJ}$ process:

$$V_J \equiv \frac{2}{s} \frac{1}{N_C^2 - 1} \sum_{a,b} \delta^{ab} p_1^\mu p_2^\nu V_{\mu\nu}^{ab} . \quad (3.2)$$

Here a and b are colour indices and $N_C = 3$. The amplitude $V_{\mu\nu}^{ab}$ represents the coupling of two gluons to the χ_c state being considered: the procedure for calculating this is outlined below. The f_g 's in (3.1) are the skewed unintegrated gluon densities of the proton at the hard scale μ , taken typically to be of the order of the produced massive state, i.e. $M_\chi/2$ in this case, and only one transverse momentum scale is taken into account by the prescription

$$\begin{aligned} Q_1 &= \min\{Q_\perp, |(\mathbf{Q}_\perp - \mathbf{p}_{1\perp})|\} \\ Q_2 &= \min\{Q_\perp, |(\mathbf{Q}_\perp + \mathbf{p}_{2\perp})|\} . \end{aligned} \quad (3.3)$$

The longitudinal momentum fractions carried by the gluons satisfy

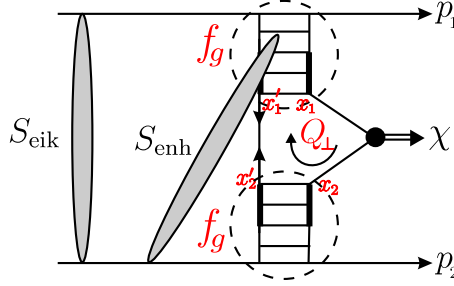


Figure 4: The perturbative mechanism for the exclusive process $pp \rightarrow p + \chi + p$, with the eikonal and enhanced survival factors shown symbolically.

$$\left(x' \sim \frac{Q_\perp}{\sqrt{s}}\right) \ll \left(x \sim \frac{M_\chi}{\sqrt{s}}\right). \quad (3.4)$$

The t dependence of the f_g 's is not well known, but in the limit that the protons scatter at small angles, we can assume a factorization of the form

$$f_g(x, x', Q_i^2, \mu^2; t) = f_g(x, x', Q_i^2, \mu^2) F_N(t), \quad (3.5)$$

where the t -dependence is isolated in a proton form factor, which we take to have the phenomenological form $F_N(t) = \exp(bt/2)$. In such a case a fit to soft hadronic data [32] gives $b \simeq 4 \text{ GeV}^{-2}$, which is also consistent with extracting $F_N(t)$ from the t -dependence in ‘elastic’ J/ψ photoproduction [41]. We will therefore use $b = 4 \text{ GeV}^{-2}$ as our value for the slope parameter throughout.

In the kinematic region specified by (3.4), the skewed unintegrated densities are given in terms of the conventional (integrated) densities $g(x, Q_i^2)$. To single log accuracy, we have⁸

$$f_g(x, x', Q_i^2, \mu^2) = R_g \frac{\partial}{\partial \log Q_i^2} [xg(x, Q_i^2) \sqrt{T_g(Q_i^2, \mu^2)}], \quad (3.6)$$

where T_g is the usual Sudakov survival factor which ensures that the active gluon does not emit additional real partons in the course of the evolution up to the hard scale μ , so that the rapidity gaps survive. R_g is the ratio of the skewed $x' \ll x$ unintegrated gluon distribution to the conventional diagonal density $g(x, Q^2)$. For $x \ll 1$ it is completely determined [43]. The explicit form for T_g is given by resumming the virtual contributions to the DGLAP equation. It is given by

$$T_g(Q_\perp^2, \mu^2) = \exp\left(-\int_{Q_\perp^2}^{\mu^2} \frac{d\mathbf{k}_\perp^2}{\mathbf{k}_\perp^2} \frac{\alpha_s(k_\perp^2)}{2\pi} \int_0^{1-\Delta} \left[zP_{gg}(z) + \sum_q P_{qg}(z)\right] dz\right). \quad (3.7)$$

Here, as in [5], we go beyond the collinear approximation and in the T factor we resum not just the single collinear logarithms, but the single soft $\ln(1-z)$ terms as well. To a good approximation, this can be achieved by taking the upper limit of the z integration in (3.7)

⁸In actual calculations, we use a more precise phenomenological form given by Eq. (26) of [42].

to be

$$\Delta = \frac{k_{\perp}}{k_{\perp} + 0.62M_{\chi}}. \quad (3.8)$$

Returning to the $gg \rightarrow \chi_c$ amplitude, we note that the original extension of the CEP formalism to χ_{c0} production in [5] was achieved in direct analogy to the Higgs case, that is by assuming that the χ_{c0} coupled to the gluons as a pure scalar with any effects from its internal structure neglected. We now wish to go beyond this approximation and model the internal structure of the χ_c meson for all three J states and in particular their coupling to two gluons. This is done by a simple extension of the calculation of [44], where the coupling of 3P_J quarkonium states to two off-mass-shell photons is considered: as the gluons are in a colour singlet state the only difference will be constant prefactors resulting from colour algebra. We will simply state the results for the three amplitudes, leaving the derivation to Appendix A:

$$V_0 = \sqrt{\frac{1}{6}} \frac{c}{M_{\chi}} ((q_{1\perp} q_{2\perp})(3M_{\chi}^2 - q_{1\perp}^2 - q_{2\perp}^2) - 2q_{1\perp}^2 q_{2\perp}^2), \quad (3.9)$$

$$V_1 = -\frac{2ic}{s} p_{1,\nu} p_{2,\alpha} ((q_{2\perp})_{\mu} (q_{1\perp})^2 - (q_{1\perp})_{\mu} (q_{2\perp})^2) \epsilon^{\mu\nu\alpha\beta} \epsilon_{\beta}^{*\chi}, \quad (3.10)$$

$$V_2 = \frac{\sqrt{2}cM_{\chi}}{s} (s(q_{1\perp})_{\mu} (q_{2\perp})_{\alpha} + 2(q_{1\perp} q_{2\perp}) p_{1\mu} p_{2\alpha}) \epsilon_{\chi}^{*\mu\alpha}, \quad (3.11)$$

where $q_{1\perp} \equiv Q_{\perp} - p_{1\perp}$ and $q_{2\perp} \equiv -Q_{\perp} - p_{2\perp}$. The amplitudes are normalised as in (3.2) and the $q_{i\perp}$ are 4-vectors with $q_{i\perp}^2 \equiv -\mathbf{q}_{i\perp}^2 < 0$ throughout.⁹ Considering first the χ_{c0} vertex, in the $\mathbf{Q}_{\perp}^2 \ll M_{\chi}^2$ limit (which is true to an acceptable degree of accuracy) we expect the internal structure of the χ_{c0} to be unimportant, and therefore to recover the previous result of [5]. We find

$$V_0 \approx \frac{48\pi\alpha_S}{\sqrt{N_C}M_{\chi}^3} \frac{\phi'_c(0)}{\sqrt{\pi M_{\chi}}} (q_{1\perp} q_{2\perp}). \quad (3.12)$$

Making use of the standard NRQCD result (see for example Refs. [45, 46, 47]),

$$\Gamma(\chi_{c0} \rightarrow gg) = 96 \frac{\alpha_S^2}{M_{\chi}^4} |\phi'_c(0)|^2, \quad (3.13)$$

⁹Four-vector scalar products are denoted by (pq) .

we find¹⁰

$$|V_0|^2 = \frac{8\pi\Gamma(\chi_{c0} \rightarrow gg)}{M_\chi^3} (q_{1\perp} q_{2\perp})^2, \quad (3.14)$$

which has the same form and normalisation as the previous result, as it must do. We will take this large M_χ limit throughout. Turning now to the χ_{c1} vertex, we can immediately see that it vanishes for on-shell gluons, that is when $q_i^2 = q_{i\perp}^2 = 0$, as dictated by the Landau-Yang theorem (see Section 2). Furthermore, in the forward limit we have $q_{1\perp} = -q_{2\perp} = Q_\perp$ and so

$$V_0 \rightarrow -\sqrt{\frac{3}{2}} c M_\chi Q_\perp^2, \quad (3.15)$$

$$V_1 \rightarrow \frac{4ic}{s} Q_\perp^2 p_{1,\nu} p_{2,\alpha} Q_{\perp\mu} \epsilon^{\mu\nu\alpha\beta} \epsilon_\beta^{*\chi}, \quad (3.16)$$

$$V_2 \rightarrow -\frac{\sqrt{2}cM}{s} (s Q_{\perp\mu} Q_{\perp\alpha} + 2Q_\perp^2 p_{1\mu} p_{2\alpha}) \epsilon_\chi^{*\mu\alpha}. \quad (3.17)$$

We see that V_1 is odd in Q_\perp , and will therefore vanish upon the loop integration (3.1) over \mathbf{Q}_\perp . For V_2 we make use of the identity

$$\int d^2 Q_\perp Q_{\perp\mu} Q_{\perp\sigma} = \frac{\pi}{2} \int dQ_\perp^2 Q_\perp^2 g_{\mu\sigma}^T, \quad (3.18)$$

where $g_{\mu\sigma}^T$, the transverse part of the metric, can be written in the covariant form

$$g_{\mu\sigma}^T = g_{\mu\sigma} - \frac{2}{s} (p_{1\mu} p_{2\sigma} + p_{1\sigma} p_{2\mu}). \quad (3.19)$$

We then find $V_2 \propto \epsilon_\mu^\mu$ which vanishes due to the tracelessness of the χ_2 polarization tensor (A.18). We see that, as expected, the χ_{c2} and χ_{c1} production amplitudes vanish in the forward limit, and we will therefore expect the corresponding rates to be suppressed relative to χ_{c0} production, via the integration over the proton form factor $e^{bt_i} \approx e^{-b\mathbf{p}_{i\perp}^2}$ which suppresses large $\mathbf{p}_{i\perp}^2$ values. In fact we can give a very rough estimate for the level of suppression we will expect. Squaring and summing over polarization states gives

$$|V_0|^2 : |V_1|^2 : |V_2|^2 \sim 1 : \frac{\langle \mathbf{p}_\perp^2 \rangle}{M_\chi^2} : \frac{\langle \mathbf{p}_\perp^2 \rangle^2}{\langle \mathbf{Q}_\perp^2 \rangle^2}. \quad (3.20)$$

Note that this result, as well as the amplitudes of (3.9 - 3.11), is also applicable to the CEP

¹⁰Analogously to Ref. [5], we assume the same NLO correction for the $gg \rightarrow \chi$ vertex as for the $\chi \rightarrow gg$ width, which can be valid only within a certain approximation. Moreover, as has been known for some time in the P -wave case (see for example Ref. [48]), the NNLO and higher-order radiative corrections to the $\chi \rightarrow gg$ transition are expected to be numerically quite large, and this would result in further uncertainties in the theoretical expectations. Recall that these corrections are not universal and depend on the spin-parity assignment of the P -wave states. In particular, it is known that in the χ_0 case the dominant part of the NLO correction comes from the $(i\pi)^2$ term originating from the Sudakov-like double logarithm $\alpha_s \ln^2(q^2/M^2)$, when the imaginary part of the logarithm ($= -i\pi$) is squared. This double logarithm, and correspondingly the $(i\pi)^2$ contributions, are absent for the case of the χ_1 , where the amplitude for on-mass-shell ($q^2 = 0$) gluons vanishes due to the Landau-Yang theorem.

of χ_b mesons. The factor of $\langle \mathbf{p}_\perp^2 \rangle$ comes from integrating over the assumed exponential form of the proton vertex,

$$\langle \mathbf{p}_\perp^2 \rangle = \int d\mathbf{p}_\perp^2 e^{-b\mathbf{p}_\perp^2} = \frac{1}{b} = \frac{1}{4} \text{ GeV}^2. \quad (3.21)$$

If for simplicity we assume $\langle \mathbf{Q}_\perp^2 \rangle \approx 1.5 \text{ GeV}^2$ and $M_\chi^2 \approx 10 \text{ GeV}^2$, we obtain¹¹

$$|V_0|^2 : |V_1|^2 : |V_2|^2 \sim 1 : \frac{1}{40} : \frac{1}{36}. \quad (3.22)$$

While it is clear that we will have a quite sizeable suppression of the χ_{c1} and χ_{c2} CEP cross sections, these values are of course only very rough estimates, and an explicit calculation is required to confirm them.

We stress again that the legitimacy of the extension of the purely perturbative QCD treatment for central exclusive Higgs production to the χ_c case is somewhat questionable. For Higgs production the hard scale μ is set by $M_H/2$, and so we expect that a reliable calculation within perturbative QCD can be performed. In particular, the Sudakov factor leads to an IR stable result, with only a small contribution to the cross section from the region of Q_\perp below $\sim 1 \text{ GeV}$ (although this is not to say the calculation does not come with significant uncertainties). However, in the case of χ_c production, where the ‘hard’ scale is $\sim 1 \text{ GeV}$, we expect and find that a significant part of the cross section comes from the IR unstable low Q_\perp region. It might seem then, that despite the attractions of considering central exclusive χ_c production, any attempt to calculate a reliable cross section within the perturbative QCD framework is unlikely to succeed. This is not the case: the philosophy we take is that, even if the purely perturbative calculation is not IR stable, we should expect a smooth matching between the perturbative regime and the ‘soft’ regime to which we can apply a non-perturbative Regge model. This was done in [5] for the χ_{c0} , with a simple model for the Pomeron invoked, and the non-perturbative and perturbative contributions were found to be of a similar size, which gives justification for the inclusion of a perturbative contribution to χ_c CEP. On the other hand, there is much uncertainty surrounding which non-perturbative models for the Pomeron are most appropriate in this context, and so results such as this can only be used as a guide.

Returning to the perturbative calculation, several comments are in order. As mentioned above, in the case of the χ_c we expect a significant proportion of the cross section to come from the low Q_\perp region where perturbation theory is not valid, and there will correspondingly be a large degree of uncertainty in its predicted value. Given our lack of detailed understanding of low Q_\perp non-perturbative gluon dynamics, the best we can do is to introduce an infrared cut-off to the Q_\perp loop integral such that we are only considering

¹¹In fact, accounting for the values of $p_{1\perp}, p_{2\perp}$ in the denominator of (3.1) we obtain a slightly larger value of the effective slope $b^{\text{eff}} = b + O(1/Q_\perp^2) > 4 \text{ GeV}^{-2}$. Therefore we expect a slightly larger suppression of the higher spin, χ_1 and χ_2 , states than that given by (3.22). Note also that for a heavier meson (χ_b) CEP the slope b^{eff} will be smaller than that for the case of χ_c due to a typically larger values of Q_\perp in the integral (3.1).

the regime where perturbation theory will be reliable. This can be loosely justified on the grounds that our current understanding of these non-perturbative dynamic predicts that the low Q_\perp contribution appears to be suppressed [49]. Nevertheless significant uncertainties remain, both in the specific choice of cut-off, for which we have rough physical guidelines but which inevitably amounts to a subjective decision, and in what contribution we would actually expect from the low Q_\perp region, which a cut-off prescription simply ignores.

A further uncertainty that is worth mentioning arises from the skewed PDFs, which we can express via (3.6) in terms of the conventional PDFs $g(x, Q^2)$, and therefore evaluate. Unfortunately, although this is in principle true, there is a large degree of uncertainty in the value of the conventional PDFs at the low x and low Q^2 scales we are considering, as can be seen in Fig. 5 where four representative PDF sets are plotted at $Q^2 = 1.5 \text{ GeV}^2$. In the case of exclusive χ_c production at the Tevatron ($\sqrt{s} = 1.96 \text{ TeV}$) we are sampling the $x \sim 2 \times 10^{-3}$ region, for which there is a large uncertainty. Recalling that the final cross section depends quartically on the skewed PDFs, this is clearly unacceptable. We can see, on the other hand, that as x is increased the uncertainty rapidly decreases and we have a reasonable agreement between the sets in the region $0.05 \lesssim x \leq 1$. We can therefore perform the cross section calculation for a lower c.m.s energy such that the sampled x value is in this range, although we must be careful that the corresponding x value is not too high, as our initial formula for the skewed PDFs relies on a small x approximation. In actual calculations a value of $\sqrt{s} = 60 \text{ GeV}$ is chosen, which corresponds to $x \sim 0.05$. To make contact with the experimental c.m.s. energies of the Tevatron we then assume that the total cross section exhibits the Regge behaviour

$$d\sigma \propto s^{\alpha_P(t_1) + \alpha_P(t_2) - 2} . \quad (3.23)$$

This gives us a simple way to avoid the large uncertainties of the PDFs in the low x region, although our final result will depend on the validity of this Regge assumption and on the specific value of the Pomeron intercept $\alpha_P(0)$ that we use.¹²

We end this section with a brief review of the uncertainties that are present in our calculation. First, we have the uncertainty in our choice of hard scale μ and the prescription (3.3) for the transverse momentum scale Q_i^2 , with for example the choice $\mu = M_H/4$ in the Higgs case giving a quoted enhancement of 30% to the cross section [4]. Further to this we have the even more considerable uncertainty coming from the dependence of the cross section on the conventional PDFs to the fourth power in the low x and Q^2 region, where they are not well determined. We also have the dependence of the final result on the non-perturbative, non-universal survival factor, which gives perhaps the largest uncertainty in the overall production rate. Differences in the higher-order QCD radiative corrections to the $gg \rightarrow \chi$ vertex could also cause additional uncertainties. Finally we have the uncertainty in the low Q_\perp contribution to the perturbative amplitude, which we find to be quite large in the χ_c case. For more details of these issues we refer the reader to [4].

¹²Our procedure is equivalent to assuming a Regge-based extrapolation of the PDFs to small x .

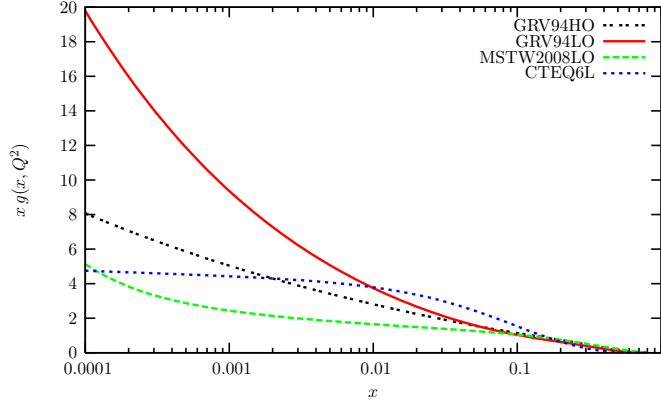


Figure 5: LO and NLO PDFs at $Q^2 = 1.5 \text{ GeV}^2$, plotted as function of x . Four representative PDF sets are displayed, and a large uncertainty at small x is clear.

4. SuperCHIC Monte Carlo Generator

In [5], central exclusive χ_{c0} meson production and its subsequent decay to $J/\psi\gamma \rightarrow \mu^+\mu^-\gamma$ was modelled using the CHIC Monte Carlo event generator, but we now wish to consider the case where higher spin χ_c states are produced. The CEP of the three $\chi_{c(0,1,2)}$ states is modelled using a new, more general, Monte Carlo programme, SuperCHIC.¹³ This follows essentially the same procedure for generating the relevant phase space as the previous CHIC MC – optimised to reduce the event weight variation – but with some important generalisations included that we will now outline.

The explicit evaluation of (3.1) is in all cases performed ‘offline’ from the SuperCHIC Monte Carlo event generator: to perform the loop integration for each event would lead to an unacceptably large run-time. The skewed PDFs are calculated as outlined in Section 3, with the Sudakov factor read in from a grid to minimise run-time, and (3.1) then evaluated using standard Monte Carlo techniques. We go beyond the approximation used in [5], where the amplitude squared was calculated in the forward limit, with the p_\perp dependence isolated in the proton form factors. Such an assumption is not relevant for the Tevatron, where the p_\perp of the final state protons is not measured [20], and so we must include non-forward effects. This will not only give a more accurate evaluation of the χ_{c0} cross section, but is also essential in the case of χ_{c1} and χ_{c2} production, where the corresponding amplitudes vanish in the forward limit. On the other hand, we still need to perform the loop integration separately from the Monte Carlo event generator. Considering first the χ_{c0} amplitude A_0 , this can be achieved by noting that for small p_\perp it must have the form

$$\begin{aligned}
 A_0 &\propto \int \frac{d^2 Q_\perp (\mathbf{q}_{1\perp} \cdot \mathbf{q}_{2\perp})}{Q_\perp^2 \mathbf{q}_1^2 \mathbf{q}_2^2} f_g(x_1, Q_1^2, \mu^2) f_g(x_2, Q_2^2, \mu^2) \\
 &\approx C_0 + C_1(\mathbf{p}_{1\perp}^2 + \mathbf{p}_{2\perp}^2) + C_{12}(\mathbf{p}_{1\perp} \cdot \mathbf{p}_{2\perp}) + \dots,
 \end{aligned} \tag{4.1}$$

¹³The extension to, for example, the CEP of pseudo-scalar η_c or higher excitation $\chi_c(nP)$ states, as well as the respective b -quark states χ_b , η_b and $\chi_b(nP)$, is planned for future work.

that is, there exists a Taylor expansion for A_0 formed from all possible scalar combinations of the $p_{i\perp}$, the validity of which depends on the suppression in p_{\perp}^2 coming from the proton form factors. Squaring (4.1) and keeping only the leading terms in $p_{i\perp}^2$, we can see that this expansion is equivalent to making the replacement (at lowest order in $p_{i\perp}^2$)

$$e^{-b\mathbf{p}_{i\perp}^2} \rightarrow e^{-(b-2\frac{C_1}{C_0})\mathbf{p}_{i\perp}^2} . \quad (4.2)$$

Thus to a first approximation we expect the inclusion of non-zero p_{\perp} in the amplitude calculation to simply result in a change in the effective slope of the proton form factor. This then allows for an easy way to take into account the effect of non-forward protons in the amplitude, as we can simply model $|A_0|^2$ as a Gaussian,

$$e^{-b(\mathbf{p}_{1\perp}^2 + \mathbf{p}_{2\perp}^2)} |A_0|^2 \propto e^{-b_0^{\text{eff}}(\mathbf{p}_{1\perp}^2 + \mathbf{p}_{2\perp}^2)} , \quad (4.3)$$

where the slope b_0^{eff} and the overall normalisation are set by matching the values of $\langle p_{\chi\perp}^2 \rangle$ and the integrated cross section, respectively, to those given by the exact expression for $|A_0|^2$. We note that the exact expression for A_0 (and therefore the $p_{\chi\perp}$ distribution) will depend in general on the azimuthal angle between the outgoing protons, but by choosing to model this effect by simple Gaussians in $p_{i\perp}^2$ the resultant azimuthal correlations between the protons will not be fully modelled in the Monte Carlo. Thus in the case of the χ_{c0} any deviation, for example, from the flat behaviour of (2.2) is ignored. On the other hand it is clear that we are not currently interested in correctly modelling the p_{\perp} distributions of the outgoing protons, which we recall are not measured at the Tevatron, but only those of the centrally produced final state particles, which it is important to know when discussing possible methods for distinguishing the three χ_c states, and the simple Gaussian approximation achieves this to an acceptable degree of accuracy.¹⁴ However, we should be careful in our application of this approximation, as no strict $Q_{\perp} \gg p_{\perp}$ hierarchy exists for the χ_c .¹⁵

The higher J states are more complicated due to their non-trivial Lorentz structure, but the basic argument remains the same. We can write the χ_{c1} and χ_{c2} amplitudes, omitting the χ_c polarization vectors etc. for simplicity, as

$$A_1^{\mu} \propto (p_{2\perp} - p_{1\perp})^{\mu} e^{-b_1^{\text{eff}}(\mathbf{p}_{1\perp}^2 + \mathbf{p}_{2\perp}^2)/2} , \quad (4.4)$$

$$A_2^{\mu\nu} \propto (s(p_{1\perp})^{\mu}(p_{2\perp})^{\nu} + 2(p_{1\perp}p_{2\perp})p_1^{\mu}p_2^{\nu}) e^{-b_2^{\text{eff}}(\mathbf{p}_{1\perp}^2 + \mathbf{p}_{2\perp}^2)/2} , \quad (4.5)$$

where we must now square the amplitudes and sum over the relevant χ_c polarization states before matching the values of the normalisation and slope as before.

SuperCHIC is a standard MC event generator that calculates the relevant weight for each generated event using these effective slopes, which can simply be read in at the

¹⁴In fact, in the case of the χ_{c2} it is necessary to include a $\mathbf{p}_{1\perp} \cdot \mathbf{p}_{2\perp}$ term in the fit. We also note that, while it is not done here, the complete inclusion of the correct azimuthal correlations, which may be relevant for measurements at the LHC with tagged forward protons, remains a possible future extension of the Monte Carlo.

¹⁵Note that such a procedure can be useful in the case of CEP of the Higgs boson [6, 12].

beginning of the run. We give the option of generating events for purely χ_{c0} , χ_{c1} and χ_{c2} production, as well as the (experimentally relevant) option of generating all three states at once. It is possible to generate the differential cross section $d\sigma/dy_\chi$ at a given rapidity y_χ value or the full cross section over a pre-specified χ_c rapidity range, with an approximate phenomenological fit invoked for the y_χ dependence of the cross section.

Having generated the appropriately weighted central exclusive χ_c event, we then generate the decay process $\chi_c \rightarrow J/\psi\gamma \rightarrow \mu^+\mu^-\gamma$ through which exclusive χ_c production has been observed at the Tevatron. While the isotropic decay of the scalar $\chi_{c0} \rightarrow J/\psi\gamma$ is trivial, the situation for χ_{c1} and χ_{c2} , which have non-trivial polarization states that must be accounted for in the relevant decays, is not so simple. The calculation of the different decay distributions is, however, relatively straightforward and is outlined in full in Appendix B. In all cases, these decays have an integrated weight of unity, while we multiply the overall cross section by the relevant branching ratios, taken from [37]. For the χ_{c1} , χ_{c2} and J/ψ we generate the spin states in the helicity basis: that is, we generate the $\chi_c(J/\psi)$ polarization vectors in the $\chi_c(J/\psi)$ rest frame, before boosting along the spin quantization (z) axis and then rotating in the $z - \mathbf{p}_{\chi(\psi)}$ plane. Finally, to improve the overall efficiency we allow as input the option of specifying values for the experimentally significant cuts on the final state $\mu^+\mu^-$ pair, in particular the maximum pseudorapidity $|\eta|$ and the minimum p_\perp . All kinematic information for the produced particles is calculated and can be read out at the end of the run.

5. Results

We begin, for the sake of comparison with the previous results of [5], with a calculation of the χ_{c0} cross section in the forward limit. As in [5], we use GRV94H0 partons [50] throughout¹⁶, and we choose the value of $Q_\perp = 0.85$ GeV as our infrared cut-off. Combining the perturbative and non-perturbative contributions, we find

$$\left. \frac{d\sigma_{\chi_{c0}}^{\text{approx}}}{dy_\chi} \right|_{y_\chi=0} = 80 \text{ nb} . \quad (5.1)$$

Once we have corrected for the revised PDG value for the total χ_{c0} width (which has decreased by a factor ~ 1.4), as well as the slightly revised value of the survival factor that we use, we find that this is in good agreement with the previous result quoted in [5]. Moreover, this is also in excellent agreement with the experimental value from the CDF collaboration [20]:

$$\left. \frac{d\sigma_{\chi_c}^{\text{exp}}}{dy_\chi} \right|_{y_\chi=0} = (76 \pm 14) \text{ nb} . \quad (5.2)$$

We emphasise that this value was *assumed*, rather than being observed, to correspond to χ_{c0} production, as the mass difference between the three χ_c states was not resolvable within the experimental set-up.

¹⁶As already mentioned, the GRV94H0 gluon PDF is very consistent with the more recent MSTW2008 and CTEQ LO and NLO gluon PDFs in the $0.05 < x < 1$ region.

We now consider the effect of non-forward protons ($p_\perp \neq 0$) on this cross section (see also [4, 6]). By directly integrating over the p_\perp dependent amplitude squared and fitting the resultant $p_{\chi_\perp}^2$ distribution according to (4.3), we find

$$b_0^{\text{eff}} = 6.6 \text{ GeV}^{-2}, \quad (5.3)$$

that is, a steepening in the effective slope of the proton form factor¹⁷. The effect of this is shown in Fig. 6, where we have plotted the differential cross section as a function of $p_\perp(\chi_{c0})$ in the forward and non-forward limits discussed above. As a check, we plot both the exact and our fitted results for the non-forward limit: we can see that the match is sufficiently accurate for our purposes. As expected, the steeper slope corresponds to $p_\perp(\chi_{c0})$ being more sharply peaked at low p_\perp values. This effect is enhanced by the prescription (3.3) for the argument Q_i^2 of the skewed PDFs. In particular, we have introduced an infrared cut-off to avoid a contribution from the low Q_\perp domain, where perturbation theory is not valid. However we can see that (3.3) will have the average effect of pushing Q_i into this ‘soft’ region which we are neglecting, and therefore lower values of p_\perp will be favoured, leading to a steepening of the effective slope. On the other hand, we could, instead of taking the minimum of the two gluon transverse momenta, take their average, which gives $b_0^{\text{eff}} \approx 5.6 \text{ GeV}^{-2}$. It is clear then that we expect some steepening in the effective slope, but the exact amount is very much tied up in the overall uncertainties of the calculation. Naïvely, we might expect this to lead to a factor of ~ 3 decrease in the production cross section, via the integration over the transverse momenta $p_{i\perp}$, however we recall (see, for example, [5, 14, 35]) that the total cross section depends on the ratio S^2/b^2 , which depends only weakly on b^2 ; that is the reduction in the cross section caused by the increased slope is largely compensated by an increase in the survival factor for the more peripheral interaction, leading to only a small overall decrease in the χ_{c0} rate. We next consider the χ_{c1} and χ_{c2} cross sections, which are calculated following the procedure outlined in Section 4. Directly integrating over the p_\perp dependent amplitude squared and fitting the resultant $p_{\chi_\perp}^2$ distribution according to (4.4) and (4.5) for χ_{c1} and χ_{c2} CEP, respectively, we find the following values for the effective slopes:

$$b_1^{\text{eff}} = 4.6 \text{ GeV}^{-2}, \quad (5.4)$$

$$b_2^{\text{eff}} = 5.9 \text{ GeV}^{-2}, \quad (5.5)$$

We can see from Fig. 3 that while the χ_{c0} and χ_{c1} eikonal survival factors are approximately constant, the χ_{c2} eikonal survival factor has a strong dependence on the p_\perp of the χ_{c2} , which we read in from a grid in the Monte Carlo. Making use of (5.3), (5.4) and (5.5) we find

$$S_{\text{eik}}^2(\chi_0) : S_{\text{eik}}^2(\chi_1) : \langle S_{\text{eik}}^2(\chi_2) \rangle \approx 0.098 : 0.15 : 0.22. \quad (5.6)$$

We emphasise that the gap survival factor S^2 depends on the effective slope b^{eff} of the *bare*

¹⁷Recall that here $b^{\text{eff}}/2$ is the slope of the ‘bare’ amplitude *before* screening effects are included. The inclusion of absorptive effects (i.e. the gap survival factor) will further enlarge the p_\perp -slope of the experimentally observed forward proton distributions.

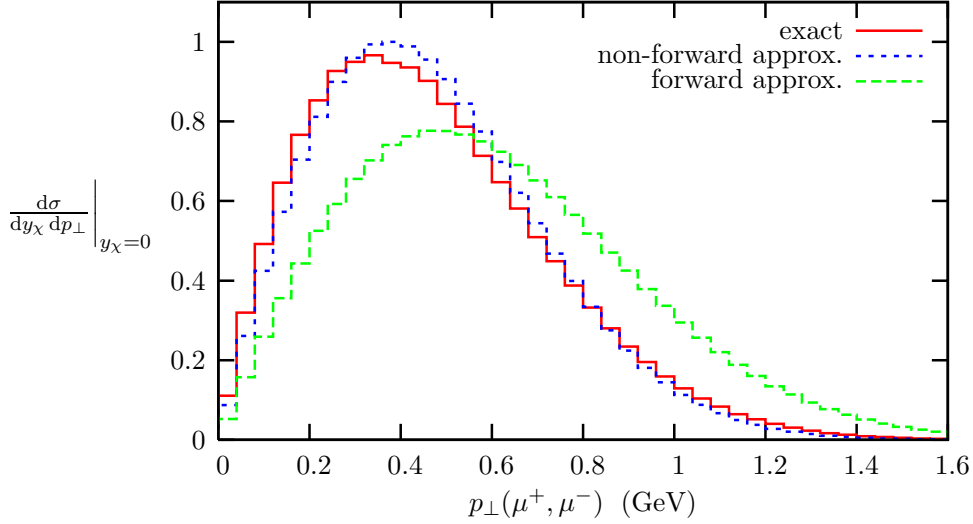


Figure 6: Differential cross section (in arbitrary units) as a function of χ_{c0} p_\perp as a result of exactly calculating the p_\perp dependent χ_{c0} amplitude (‘exact’), setting $p_\perp = 0$ in the initial amplitude calculation (‘forward approximation’) and approximating the non-forward effects by an effective slope parameter b_{eff} (‘non-forward approximation’).

(non-screened) CEP amplitude which, in turn, depends explicitly on the p_\perp of the outgoing protons, see [6]. In particular, at $b = 4 \text{ GeV}^{-2}$ we obtain $S_{\text{eik}}^2 = 0.046$, while in the case of CEP of the χ_{c0} , where $b_{\text{eff}}^0 = 6.6 \text{ GeV}^{-2}$, we obtain the value $S_{\text{eik}}^2 = 0.098$, i.e. a factor of two larger. As discussed above, such an increase in S^2 largely compensates the decrease in the CEP cross section caused by a smaller phase space in p_\perp occupied by the final state protons (due to a larger b^{eff}). Recalling that the CEP event rate depends on the ratio S^2/b^2 (rather than on S^2) [5], this can serve as a warning regarding the conclusions made in Refs. [51, 52] about the CEP rates based solely on the evaluations of S^2 for protons with $p_\perp = 0$. In addition, we have already shown in Section 3 that neglecting the $p_\perp \neq 0$ effects in the structure of the hard production subprocess can lead to a significant underestimate in the production rate of states with J^P other than 0^+ . Returning to the calculation of the higher spin χ_c cross sections we find, by including the relevant branching ratios (evaluated at rapidity $y_\chi = 0$ in all cases),

$$\frac{\Gamma_{J/\psi\gamma}^{\chi_0}}{\Gamma_{\text{tot}}^{\chi_0}} \frac{d\sigma_{\chi_{c0}}^{\text{pert}}}{dy_\chi} : \frac{\Gamma_{J/\psi\gamma}^{\chi_1}}{\Gamma_{\text{tot}}^{\chi_1}} \frac{d\sigma_{\chi_{c1}}^{\text{pert}}}{dy_\chi} : \frac{\Gamma_{J/\psi\gamma}^{\chi_2}}{\Gamma_{\text{tot}}^{\chi_2}} \frac{d\sigma_{\chi_{c2}}^{\text{pert}}}{dy_\chi} \approx 1 : 0.8 : 0.6. \quad (5.7)$$

Thus, within the perturbative framework, the expected contributions of the three χ_c states to the Tevatron data are of comparable size, despite the initial suppression in the χ_{c1} and χ_{c2} production amplitudes. The previous assumption that the Tevatron events correspond to purely χ_{c0} CEP may therefore be unjustified. To give a prediction for the total cross section we must take into account the so-called ‘enhanced’ absorptive effects, which break the soft-hard factorization previously assumed in the evaluation of the χ_{c0} CEP cross section in [5]. The generalisation of the simple two channel eikonal model to include these

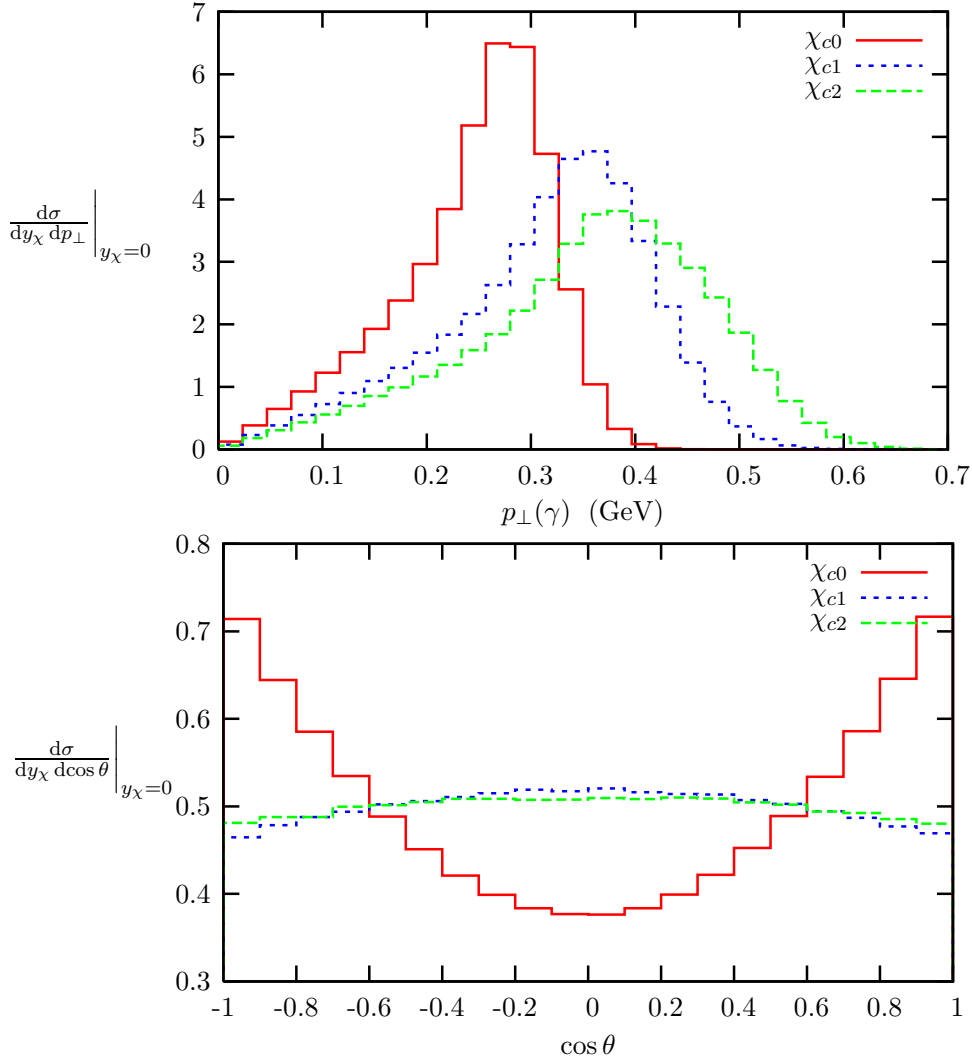


Figure 7: χ_{c0} , χ_{c1} and χ_{c2} differential cross sections, without experimental cuts, as a function of the photon p_\perp and $\cos\theta$, where θ is the angle between the μ^+ momentum in the J/ψ rest frame and the direction of the Lorentz boost from the J/ψ rest frame to the lab frame. Integrated cross sections normalised to unity before cuts are imposed in all cases.

enhanced rescattering effects is outlined in [35], where the effect of including both eikonal and enhanced screening corrections, as well as non-forward outgoing protons in the hard matrix element, can be roughly accounted for by the introduction of an ‘effective’ survival factor S_{eff}^2 . Recalling (1.1), it is found that the effect of enhanced absorption for the CEP of the light χ_c is quite strong (see also [36, 51, 52]). In particular, ignoring for simplicity any impact parameter \mathbf{b} dependence, we have

$$\langle S_{\text{eff}}^2 \rangle \approx \langle S_{\text{enh}}^2 \rangle \times \langle S_{\text{eik}}^2 \rangle \approx \frac{1}{3} \langle S_{\text{eik}}^2 \rangle, \quad (5.8)$$

with the enhanced survival factor S_{enh}^2 (at our present level of understanding) approxi-

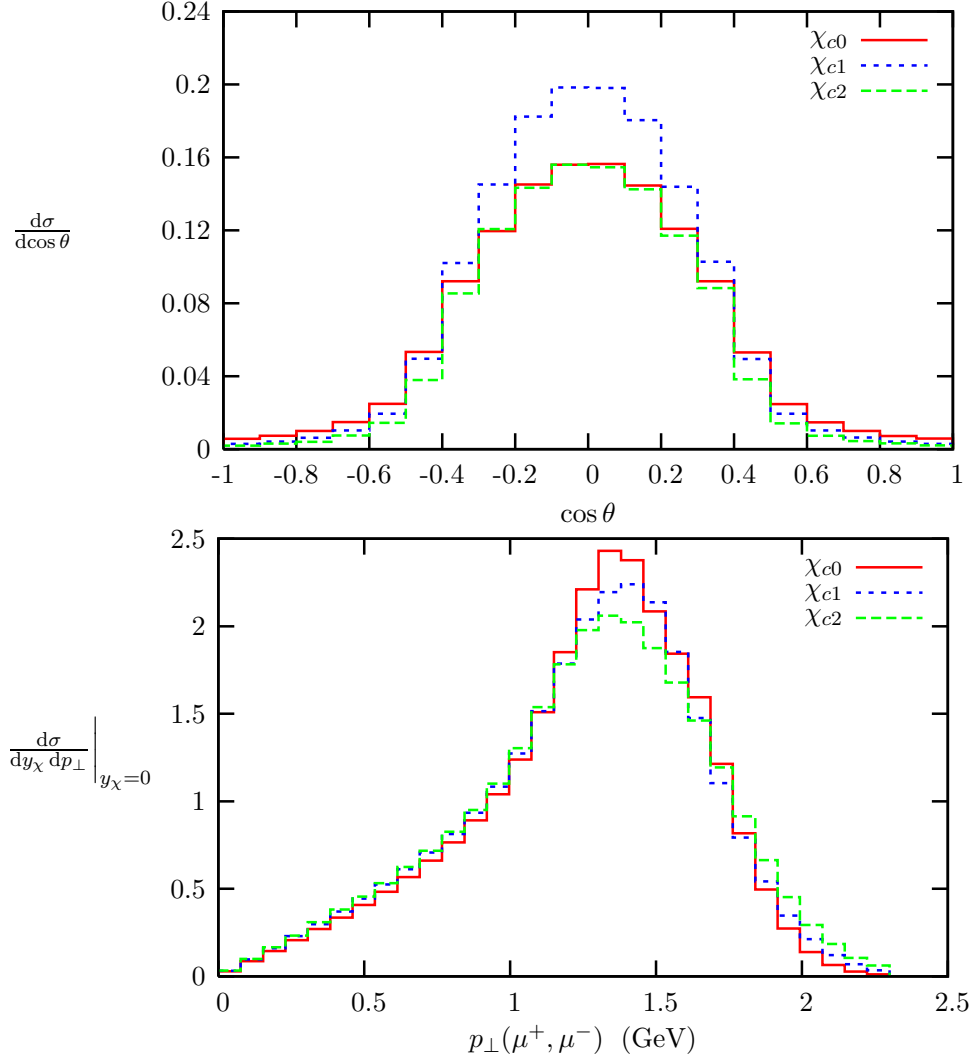


Figure 8: Differential cross sections as a function of $\cos\theta$, with experimental cuts, and the μ^+, μ^- p_\perp , without experimental cuts. Integrated cross sections normalised to unity before cuts are imposed in all cases.

mately the same for all three χ_c states. Multiplying by this suppression factor and including the contribution from the three J states to the observed cross section, we can then use the branching ratio $\text{Br}(\chi_{c0} \rightarrow J/\psi + \gamma)$, as was done for the CDF data, to produce a rough value for the ‘ χ_{c0} ’ cross section at Tevatron energies (prior to any corrections due to the varying experimental acceptances of the χ_c states),

$$\left.\frac{d\sigma_{\chi_c}^{\text{tot}}}{dy_\chi}\right|_{y_\chi=0} \approx 65 \text{ nb} . \quad (5.9)$$

Here we stress that a sizeable proportion of the observed events are predicted to correspond to χ_{c1} and χ_{c2} CEP. Thus, the combination of including the more general enhanced rescat-

tering effects, which leads to a reduction in the predicted rate, and the contribution of the higher spin χ_{c1} and χ_{c2} states, which leads to an increase in the predicted rate, leaves the perturbative prediction for the total χ_c cross section at the Tevatron largely unchanged and, crucially, still in good agreement with the experimental data.

At this point we need also to consider the non-perturbative contribution to the cross section. Leaving the explicit evaluation for future work, we simply note that the previous calculations of [53, 54] show that the non-perturbative contributions of the three χ_c states are also comparable, with the general results of Section 2 suggesting that, at least for the χ_{c0} and χ_{c1} , they will have a similar p_\perp dependence to that outlined in Section 4. We can therefore reasonably assume that the relative values of (5.7) are approximately correct. However, given the overall uncertainty in the perturbative and non-perturbative cross section calculations, we note that the precise ratio of the χ_c cross sections cannot be stated with certainty at this time. While our results suggest that some fraction of the 65 ± 10 candidate ‘ χ_{c0} ’ events observed at CDF are in fact χ_{c1} or χ_{c2} events, we can make no definitive prediction for their precise relative contributions.

In fact, we have noted that the perturbative contribution to χ_{c2} CEP is strongly suppressed due to the $J_z = 0$ selection rule, for which it decouples from two real gluons. However, for the non-perturbative contribution we have no such selection rule, and we therefore cannot exclude the possibility that the χ_{c2} non-perturbative contribution is dominant. The above-mentioned Pomeron models suggest that this may be the case, although there remains a large degree of uncertainty in how to perform these calculations, and in particular which model of the Pomeron to choose.

Putting aside the question of normalisation, we might hope to be able to distinguish between the three states by studying the angular and kinematical distributions of the final state particles as modelled in SuperCHIC, which should not depend strongly on the overall production rate. In Fig. 7 we show the polar angular distributions of the $\mu^+\mu^-$ pair and the p_\perp distributions of the photon for the three χ states, as given by SuperCHIC. For the p_\perp distribution we can see the clear separation in the χ masses coming from the position of the Jacobian peaks as p_\perp approaches the photon energy $E_\gamma \sim M_\chi - M_\psi$, although in the current experimental set-up we know it is not possible to resolve this separation.

The angular distribution is more interesting: there is clearly a significant difference between the χ_{c0} and the χ_{c1} and χ_{c2} cases with, as expected from helicity conservation, the χ_{c0} decaying into purely transversely polarized J/ψ ’s, while this is not the case for the χ_{c1} and χ_{c2} . This in principle provides a way to determine if χ_{c1} and χ_{c2} mesons are being produced, irrespective of the particular mass resolution of the experiment. Unfortunately, this does not appear to be the case in practice, as we have yet to include the experimental cuts on the kinematics of the final state particles. At CDF we require in particular that the muon pseudorapidity $|\eta| < 0.6$ and the muon $p_\perp > 1.4$ GeV. In Fig. 8 we show the angular distribution as before but with these cuts introduced, and immediately we can see that the clear difference in shape has not survived. We also show the p_\perp distribution of the muons, from which it is clear that a sizeable fraction of the events will not pass the cuts (recalling that the cut must be passed by both muons), and the pseudorapidity cut further enhances this effect. Moreover, in the low (high) θ region the $\mu^{+(-)}$ will be directed

along the motion of the J/ψ with high p_\perp , while the $\mu^{-(+)}$ will be directed against the motion of the J/ψ and will therefore have low p_\perp . This is clear from Fig. 8 where the $\cos\theta \approx +1, -1$ events which would have allowed us to distinguish between $\chi_{c1,2}$ and χ_{c0} production have not been accepted. We note that other potentially interesting variables, such as the difference in the azimuthal angle of the muons $\Delta\phi_{\mu\mu}$, appear to be equally unpromising. It therefore seems that it will be very hard, given the experimental set up and the low statistics available at the present time, to distinguish between the three χ_c states via the experimentally considered decay chain, although with more detailed analysis and/or higher statistics this conclusion may change. Another potential solution to this issue could be to consider a different decay chain, for example the direct decay of the χ_c to charged hadrons, etc. (see Section 6 below).

Finally, we can also see that the χ_{c1} has a slightly higher acceptance, with in particular (at $y_\chi = 0$)

$$\frac{d\sigma_{\chi_{c0}}^{\text{cuts}}}{d\sigma^{\text{tot}}} : \frac{d\sigma_{\chi_{c1}}^{\text{cuts}}}{d\sigma^{\text{tot}}} : \frac{d\sigma_{\chi_{c2}}^{\text{cuts}}}{d\sigma^{\text{tot}}} \approx 16\% : 17\% : 15\% . \quad (5.10)$$

The acceptance is therefore reasonably uniform, and so should not present a significant obstacle when considering χ_{c1} and χ_{c2} production experimentally.

6. Summary and Outlook

Motivated by the recent experimental observation of exclusive χ_c events at the Tevatron, we have updated the earlier studies of central exclusive scalar χ_{c0} meson production to include χ_{c1} and χ_{c2} mesons. Due to the low scale, $M_{\chi_c}/2$, and very large rapidity gap coverage ($\Delta\eta \simeq 7.4$ units) in the CDF measurement [20], the contamination from processes in which the incoming protons dissociate is relatively small. The CDF χ_c event selection therefore effectively ensures that they come from the exclusive reaction, $p\bar{p} \rightarrow p + \chi_c + \bar{p}$.

Although χ_{c0} production was previously assumed to be dominant, we find that the χ_{c0} , χ_{c1} and χ_{c2} rates for the experimentally considered $\chi_c \rightarrow J/\psi\gamma \rightarrow \mu^+\mu^-\gamma$ decay process are in fact comparable. We have developed a new Monte Carlo event generator, SuperCHIC, which models the central exclusive production of the three χ_c states via this decay chain, and have used this to explore possible ways of distinguishing them, given that their mass differences are not resolvable within the current experimental set-up. Although we find that the severity of current experimental cuts appears to preclude this discrimination, the acceptance does not change crucially between the three states and so our conclusions regarding the overall rates remain unchanged. This therefore raises the interesting possibility that exclusive χ_{c1} and χ_{c2} production has already been observed at the Tevatron. Higher statistics and/or a broader acceptance coverage for the photon and leptons could help discriminate between the χ_c mesons via differences in the angular correlations between the final-state particles. We note also that the addition of forward proton detectors would certainly allow discrimination between the different C -even states via the measurement of the relative azimuthal angular distribution between the outgoing protons.

To further resolve the spin-parity assignment issue in the absence of forward proton detectors, it would be instructive to observe central exclusive χ_c production in other decay

channels, in particular $\pi\pi$ or $K\bar{K}$, see [5]. These modes are ideally suited for spin-parity analysis: the $\pi\pi$ or $K\bar{K}$ decay modes of the χ_{c0} meson have a branching fraction of about 1%, while these decay channels are forbidden for χ_{c1} and suppressed by about a factor of 5 for the χ_{c2} relative to the χ_{c0} , in contrast to the χ_{c2} relative enhancement for the $J/\psi\gamma$ channel. Another interesting mode for discriminating between the CEP of different χ_c states is $\chi_c \rightarrow p\bar{p}$, since the branching fraction for χ_{c0} ($\simeq 0.024\%$) is a factor of 3 higher than that for $\chi_{c1,2}$ [37]. The $\Lambda\bar{\Lambda}$ mode (branching fraction for $\chi_{c0} \simeq 0.034\%$) could also be important for spin-parity analyzing.¹⁸

In the case of two-body final states ($\pi\pi$, KK , $p\bar{p}$) where the very forward protons are not detected, further cuts can be imposed to reduce the contribution of events where the protons dissociate (via single and double diffractive dissociation). These include, for example, cuts on the transverse momentum of the resonance and on the final particles' acoplanarity angle (in the frame where the rapidity of the resonance is zero).¹⁹

In this paper we have focused on χ_c meson production at the Tevatron. It is of course straightforward to extend our results to the LHC, and we will consider this in a future study [57]. Note that we do not expect the χ_c CEP rate to have a strong energy dependence when going from the Tevatron to the LHC. The growth of the bare amplitude caused by the increase in the gluon density at smaller x is compensated by a smaller gap survival factor at the larger LHC energies, especially S_{enh}^2 , the value of which decreases due to the larger rapidity interval available for the 'enhanced' absorptive corrections, see Fig. 1(d). Indeed, the measurement of the ratios of the CEP rates at the two different (Tevatron and LHC) collider energies could allow the effects of enhanced absorption to be probed, since in these cross section ratios various uncertainties (for example, NLO corrections to the $gg \rightarrow \chi$ transition etc.) would cancel out.

The issue of forward proton detection is more relevant at the LHC (in particular for χ_b states) as the planned near-beam proton detectors, see Refs. [11, 15, 58], would allow us to measure the outgoing very forward protons. As we have already noted, the azimuthal angle distributions would provide interesting additional information with which we could discriminate between different J^{PC} states as well as investigate the dynamics of the survival factors S^2 . Moreover, as pointed out in [40], measuring the transverse momentum and azimuthal angle correlations between the outgoing protons would allow us to probe the proton opacity $\Omega(s, b_t)$ and perform a detailed test of the *whole* diffractive formalism. Even before the forward proton detectors become operational, a broad programme of heavy quarkonium studies can be performed with the existing LHC detectors (ALICE, ATLAS, CMS and LHCb), especially if the rapidity gap coverage is increased by using forward shower counters (FSC) along the beam line [59], thereby allowing detection and triggering on rapidity gaps in diffractive events.

In future work we will also consider χ_b and $\eta_{b,c}$ meson CEP and include them in the

¹⁸Rough estimates show that the background from continuum $\pi\pi$, $K\bar{K}$, $p\bar{p}$ and $\Lambda\bar{\Lambda}$ central production should be quite manageable. This is in accord with measurements in two-photon collisions [55], where the $\chi_{c0,2}$ resonances decaying to $\pi\pi$ and $K\bar{K}$ final states are clearly seen.

¹⁹This procedure is similar to that used in the separation of exclusive lepton-pair production via photon-photon fusion, $pp \rightarrow p + l^+l^- + p$, see [56] for more details.

Monte Carlo. The perturbative χ_{b0} CEP rate was calculated in [3, 5] analogously to the χ_{c0} . While the higher M_χ scale results in a more perturbatively reliable prediction, the reduced rate suggests that exclusive χ_b production, observed through the $\chi_b \rightarrow \Upsilon(1S)\gamma \rightarrow \mu^+\mu^-\gamma$ decay chain, may only be relevant at the LHC. The experimental values for the $\chi_{bJ} \rightarrow \Upsilon(1S)\gamma$ branching ratios carry larger uncertainties, but a similar hierarchy to the χ_c case is observed, and so the contribution of higher spin states should once again be considered, with in particular the result of (3.20) for the relative rates remaining valid. However, we note that the higher mass scale will result in a stronger suppression of the higher spin states relative to the χ_{b0} than in the χ_c case. In particular, for χ_{b1} production we have an explicit factor of M_χ^2 in the denominator of (3.20), while the larger expected value of $\langle Q_\perp^2 \rangle$ will result in a stronger suppression of the χ_{b2} state.

The $\eta_{c,b}$ CEP cross sections can be calculated by using the same formalism as for the χ mesons, the only difference being that for the $L = 0$ quarkonium state the $gg \rightarrow \eta$ vertex is proportional to the value of the wave function $\phi(0)$ at the origin and not to $\phi'(0)$ as in (3.12). The vertex V_η should therefore be normalised to the leptonic width of the J/ψ (or Υ for η_b) decay – the vector mesons from the same $L = 0$ multiplet. Note also that for the heavier χ_b or η_b mesons we expect a slightly lower slope b^{eff} (due to a larger mean $\langle Q_\perp^2 \rangle$) and a larger value of S_{enh}^2 (due to a smaller rapidity interval available for the ‘enhanced’ absorptive corrections, Fig. 1(d)). Preliminary estimates indicate that the η_c CEP rate (which we recall from [4] will be proportional to $\langle p_{1\perp}^2 p_{2\perp}^2 \rangle / \langle Q_\perp^2 \rangle^2$) is expected to be about two orders of magnitude lower than in the χ_{c0} case.

We are also planning to revisit $\gamma\gamma$ CEP in a wider interval of photon E_T , rapidity and di-photon mass M than that considered in [23] and to include this in the Monte Carlo generator. Note that the measurement of the ratio of $\gamma\gamma$ CEP at $E_T = 5$ GeV to that of χ_b production may allow us to reduce various uncertainties in the calculations, with in particular the dependence on the survival factors cancelling out.

Finally, we note that the spin-parity analyzing properties of central exclusive production could shed light on the dynamics of the *zoology* of ‘exotic’ charmonium-like states (X, Y, Z) which have been discovered in the last few years (see for example [37, 60]), and whose nature and in many cases spin-parity assignment still remain unclear.

Acknowledgements

We thank Albert De Roeck, Aliosha Kaidalov, Alan Martin, Risto Orava, Jim Pinfold, Rainer Schicker, Oleg Teryaev, and especially Mike Albrow for useful and encouraging discussions. MGR, LHL and WJS thank the IPPP at the University of Durham for hospitality. The work was supported by grant RFBR 07-02-00023, by the Russian State grant RSGSS-3628.2008.2. LHL acknowledges financial support from the University of Cambridge Domestic Research Studentship scheme.

A. $\chi_c \rightarrow gg$ amplitudes

A.1 χ_{c0}

We use the formalism of [44] and the kinematics of Section 3 throughout. The general colour-averaged vertex for the coupling to two gluons has the form

$$V_0 \equiv \epsilon_1^\alpha \epsilon_2^\beta V_{\alpha\beta}^0 = \sqrt{\frac{1}{6}} \frac{c}{M} (I_1^0 (M^2 + (q_1 q_2)) - 2I_2^0) , \quad (\text{A.1})$$

where $\epsilon_{1,2}$ are the polarization vectors of the incoming gluons and

$$q_1 = x_1 p_1 + Q_\perp - p_{1\perp} , \quad (\text{A.2})$$

$$q_2 = x_2 p_2 - Q_\perp - p_{2\perp} , \quad (\text{A.3})$$

while we define

$$I_1^0 = F_{\mu\nu}^1 F^{2,\mu\nu} , \quad (\text{A.4})$$

$$I_2^0 = q_1^\nu F_{\mu\nu} F^{2,\mu\sigma} q_{2,\sigma} . \quad (\text{A.5})$$

Here $F_{\mu\nu}$ is the usual field strength tensor for the gluons and

$$c = \frac{1}{2\sqrt{N_C}} \frac{4g_s^2}{(q_1 q_2)^2} \sqrt{\frac{6}{4\pi M}} \phi'_c(0) , \quad (\text{A.6})$$

where g_s is the strong coupling and $\phi'_c(0)$ is the derivative of the χ_c radial wavefunction at the origin. Note that our definition of c differs from that of Ref. [44] by a factor

$$\langle 3i; \bar{3}k | 1 \rangle t_{ij}^a t_{jk}^b = \frac{\delta^{ab}}{2\sqrt{N_C}} \rightarrow \frac{1}{2\sqrt{N_C}} , \quad (\text{A.7})$$

where $\langle 3i; \bar{3}k | 1 \rangle$ is the colour space Clebsch-Gordon coefficient for the colour singlet quark configuration, and we have averaged over the gluon colour indices a, b in the last step. Recalling (3.2), we make the replacement $\epsilon_1^\mu \epsilon_2^\nu V_{\mu\nu} \rightarrow \frac{2}{s} p_1^\mu p_2^\nu V_{\mu\nu}$ and use the gauge invariance of $V_{\mu\nu}$ to give

$$I_1^0 = 2(q_{1\perp} q_{2\perp}) , \quad (\text{A.8})$$

$$I_2^0 = q_{1\perp}^2 q_{2\perp}^2 . \quad (\text{A.9})$$

Here we have made use of the identity

$$(q_1 q_2) = \frac{1}{2} (M^2 - q_{1\perp}^2 - q_{2\perp}^2) . \quad (\text{A.10})$$

We therefore obtain

$$V_0 = \sqrt{\frac{1}{6}} \frac{c}{M_\chi} ((q_{1\perp} q_{2\perp}) (3M_\chi^2 - q_{1\perp}^2 - q_{2\perp}^2) - 2q_{1\perp}^2 q_{2\perp}^2) \quad (\text{A.11})$$

A.2 χ_{c1}

The general colour-averaged vertex has the form

$$V_1 = -\frac{ic}{2}(I_1^1 + I_2^1) , \quad (\text{A.12})$$

where

$$I_1^1 = \epsilon^{\mu\nu\alpha\beta} \epsilon_\beta^{\chi*} F_{\mu\nu}^1 F_{\alpha\gamma}^2 q_2^\gamma \quad (\text{A.13})$$

$$I_1^2 = \epsilon^{\mu\nu\alpha\beta} \epsilon_\beta^{\chi*} F_{\mu\nu}^2 F_{\alpha\gamma}^1 q_1^\gamma . \quad (\text{A.14})$$

Here ϵ_β^χ is the χ_1 polarization vector and $\epsilon^{\mu\nu\alpha\beta}$ is the antisymmetric Levi-Civita tensor. This gives

$$V_1 = -\frac{2ic}{s} \epsilon^{\mu\nu\alpha\beta} \epsilon_\beta^{\chi*} p_{1,\nu} p_{2,\alpha} ((q_{2\perp})_\mu (q_{1\perp})^2 - (q_{1\perp})_\mu (q_{2\perp})^2) . \quad (\text{A.15})$$

A.3 χ_{c2}

The general colour-averaged vertex has the form

$$V_2 = -c\sqrt{2}MI_2^2 , \quad (\text{A.16})$$

where

$$I_2^2 = \epsilon_\chi^{*\mu\alpha} F_\mu^{1\beta} F_{\alpha\beta}^2 . \quad (\text{A.17})$$

$\epsilon_\chi^{\mu\alpha}$ is the χ_2 polarization tensor, which satisfies

$$\epsilon_{\mu\nu} = \epsilon_{\nu\mu} , \quad \epsilon_\mu{}^\mu = 0 , \quad \epsilon_{\mu\nu} P_\chi^\mu = 0 , \quad (\text{A.18})$$

$$\sum_{pol} \epsilon_{\mu\nu} \epsilon_{\alpha\beta}^* = \frac{1}{2} (\mathbb{P}_{\mu\alpha} \mathbb{P}_{\nu\beta} + \mathbb{P}_{\mu\beta} \mathbb{P}_{\nu\alpha}) - \frac{1}{3} \mathbb{P}_{\mu\nu} \mathbb{P}_{\alpha\beta} , \quad (\text{A.19})$$

$$\mathbb{P}^{\mu\nu} \equiv -g^{\mu\nu} + \frac{P_\chi^\mu P_\chi^\nu}{M^2} . \quad (\text{A.20})$$

We therefore obtain

$$V_2 = \frac{\sqrt{2}cM}{s} (s(q_{1\perp})_\mu (q_{2\perp})_\alpha + 2(q_{1\perp} q_{2\perp}) p_{1\mu} p_{2\alpha}) \epsilon_\chi^{*\mu\alpha} . \quad (\text{A.21})$$

B. χ_c and J/ψ decay amplitudes

We will make use of the identities

$$\epsilon^{\mu\nu\alpha\beta} \epsilon_{\tilde{\mu}\tilde{\nu}\alpha\beta} = -4 \delta_{\tilde{\mu}}^{[\mu} \delta_{\tilde{\nu}}^{\nu]} , \quad (\text{B.1})$$

$$\epsilon^{\mu\nu\alpha\beta} \epsilon_{\tilde{\mu}\tilde{\nu}\tilde{\alpha}\beta} = -3! \delta_{\tilde{\mu}}^{[\mu} \delta_{\tilde{\nu}}^{\nu} \delta_{\tilde{\alpha}}^{\alpha]} , \quad (\text{B.2})$$

$$\epsilon^{\mu\nu\alpha\beta} \epsilon_{\tilde{\mu}\tilde{\nu}\tilde{\alpha}\tilde{\beta}} = -4! \delta_{\tilde{\mu}}^{[\mu} \delta_{\tilde{\nu}}^{\nu} \delta_{\tilde{\alpha}}^{\alpha} \delta_{\tilde{\beta}}^{\beta]} . \quad (\text{B.3})$$

B.1 $\chi_c(0^{++}) \rightarrow J/\psi + \gamma$

The scalar χ_0 decays into a transversely polarized photon with a uniform angular distribution in its rest frame, and conservation of angular momentum therefore requires the J/ψ to be transversely polarized.

B.2 $\chi_c(1^{++}) \rightarrow J/\psi + \gamma$

The amplitude that is expected to dominate (as it is the amplitude which corresponds to the dipole transition [44]) is of the form

$$A_1 \sim \epsilon^{\mu\nu\alpha\beta} \epsilon_\mu^\chi \epsilon_\nu^{\psi*} p_\alpha^\gamma \epsilon_\beta^{\gamma*} . \quad (\text{B.4})$$

Squaring and summing over photon polarizations, and making use of (B.2), we find

$$\sum_{\epsilon_\gamma} |A_1|^2 \sim |(p_\gamma \epsilon_\psi)|^2 + |(p_\gamma \epsilon_\chi)|^2 + 2 \text{Re}[(\epsilon_\chi \epsilon_\psi)(\epsilon_\chi^* p_\gamma)(p_\gamma \epsilon_\psi^*)] . \quad (\text{B.5})$$

The normalisation is given by summing over J/ψ polarizations and making use of (B.1) and (B.3)

$$|A_1^{\text{norm}}|^2 \sim |(\epsilon_\chi p_\gamma)|^2 + \frac{(p_\gamma p_\psi)}{M_\psi^2} ((p_\gamma p_\psi) + 2 \text{Re}[(\epsilon_\chi^* p_\gamma)(\epsilon_\chi p_\psi)]) . \quad (\text{B.6})$$

We then divide by the normalisation factor to give the relative amplitudes squared for the three different χ_1 polarizations.

B.3 $\chi_c(2^{++}) \rightarrow J/\psi + \gamma$

Following similar arguments to the χ_1 case (that is, assuming the dipole transition dominates), we can write the invariant amplitude as

$$A_2 = \epsilon_\chi^{\mu\alpha} (F^\gamma)^\beta{}_\mu (F^\psi)_{\alpha\beta} . \quad (\text{B.7})$$

To study angular correlations it is necessary to consider the explicit form of the χ_2 polarization tensor. This represents the irreducible tensor operator for $J = 2$ angular momentum, which can be decomposed in terms of the spin and orbital polarization vectors [44]

$$\epsilon_{\mu\nu}^{(J_Z)} = \sum_{S_Z, m} \epsilon_\mu^{(S_Z)} \epsilon_\nu^{(m)} \langle S = 1, L = 1, S_Z, m | J = 2, J_Z \rangle , \quad (\text{B.8})$$

where $\langle S = 1, L = 1, S_Z, m | J = 2, J_Z \rangle$ are the Clebsch-Gordon coefficients and $\epsilon_\mu^{(S_Z)}, \epsilon_\nu^{(m)}$ have the usual explicit representation in (say) the χ_2 rest frame. We can thus decompose

the 5 polarization states as

$$\epsilon_{\mu\nu}^{+2} = \epsilon_{\mu}^{+} \epsilon_{\nu}^{+} , \quad (\text{B.9})$$

$$\epsilon_{\mu\nu}^{+1} = \sqrt{\frac{1}{2}} (\epsilon_{\mu}^{+} \epsilon_{\nu}^0 + \epsilon_{\mu}^0 \epsilon_{\nu}^{+}) , \quad (\text{B.10})$$

$$\epsilon_{\mu\nu}^0 = \sqrt{\frac{1}{6}} (\epsilon_{\mu}^{+} \epsilon_{\nu}^{-} + 2 \epsilon_{\mu}^0 \epsilon_{\nu}^0 + \epsilon_{\mu}^{-} \epsilon_{\nu}^{+}) , \quad (\text{B.11})$$

$$\epsilon_{\mu\nu}^{-1} = \sqrt{\frac{1}{2}} (\epsilon_{\mu}^{-} \epsilon_{\nu}^0 + \epsilon_{\mu}^0 \epsilon_{\nu}^{-}) , \quad (\text{B.12})$$

$$\epsilon_{\mu\nu}^{-2} = \epsilon_{\mu}^{-} \epsilon_{\nu}^{-} . \quad (\text{B.13})$$

Returning to (B.7), we obtain

$$\begin{aligned} \sum_{\epsilon_{\gamma}} |A_2|^2 &\sim 2 \text{Re} [\epsilon^{\mu\alpha} \epsilon^{*\nu\sigma} p_{\mu}^{\gamma} ((p_{\gamma} p_{\psi}) \epsilon_{\sigma}^{\psi} - (p_{\gamma} \epsilon_{\psi}) p_{\sigma}^{\psi}) (\epsilon_{\alpha}^{*\psi} p_{\nu}^{\psi} - \epsilon_{\nu}^{*\psi} p_{\alpha}^{\psi})] \\ &\quad - \epsilon^{\mu\alpha} \epsilon^{*\nu\sigma} (g_{\mu\nu} ((p_{\gamma} p_{\psi}) \epsilon_{\alpha}^{\psi*} - (p_{\gamma} \epsilon_{\psi}^{*}) p_{\alpha}^{\psi}) ((p_{\gamma} p_{\psi}) \epsilon_{\sigma}^{\psi} - (p_{\gamma} \epsilon_{\psi}) p_{\sigma}^{\psi}) \\ &\quad + p_{\mu}^{\gamma} p_{\nu}^{\gamma} (M_{\psi}^2 \epsilon_{\alpha}^{*\psi} \epsilon_{\sigma}^{\psi} - p_{\alpha}^{\psi} p_{\sigma}^{\psi})) , \end{aligned} \quad (\text{B.14})$$

where the normalisation is given by

$$|A_2^{\text{norm}}|^2 \sim \epsilon^{\mu}_{\alpha} \epsilon^{*\alpha\nu} ((p_{\gamma} p_{\psi})^2 g_{\mu\nu} + M_{\chi}^2 p_{\mu}^{\gamma} p_{\nu}^{\gamma}) + 2(p_{\gamma} p_{\psi}) p_{\mu}^{\gamma} p_{\nu}^{\gamma} \text{Re} [\epsilon^{\mu}_{\alpha} \epsilon^{*\alpha\nu}] . \quad (\text{B.15})$$

References

- [1] D. Robson, Nucl. Phys. **B130** (1977) 328;
F.E. Close, Rept. Prog. Phys. **51** (1988) 833.
- [2] P. Minkowski, Fizika B **14** (2005) 79 [arXiv:hep-ph/0405032].
- [3] V. A. Khoze, A. D. Martin and M. G. Ryskin, Eur. Phys. J. C **19**, 477 (2001) [Erratum-ibid. C **20**, 599 (2001)] [arXiv:hep-ph/0011393].
- [4] A. B. Kaidalov, V. A. Khoze, A. D. Martin and M. G. Ryskin, Eur. Phys. J. C **31**, 387 (2003) [arXiv:hep-ph/0307064].
- [5] V. A. Khoze, A. D. Martin, M. G. Ryskin and W. J. Stirling, Eur. Phys. J. C **35**, 211 (2004) [arXiv:hep-ph/0403218].
- [6] A. Kaidalov *et al.*, V.A. Khoze, A.D. Martin and M. Ryskin, *Eur. Phys. J. C* **33** (2004) 261, hep-ph/0311023.
- [7] E. Klempt and A. Zaitsev, Phys. Rept. **454** (2007) 1 [arXiv:0708.4016 [hep-ph]].
- [8] F. E. Close and A. Kirk, Phys. Lett. B **397** (1997) 333 [arXiv:hep-ph/9701222];
F. E. Close, A. Kirk and G. Schuler, Phys. Lett. B **477** (2000) 13 [arXiv:hep-ph/0001158].
- [9] S. Heinemeyer, V. A. Khoze, M. G. Ryskin, W. J. Stirling, M. Tasevsky and G. Weiglein, Eur. Phys. J. C **53** (2008) 231 [arXiv:0708.3052 [hep-ph]].
- [10] V. A. Khoze, A. D. Martin and M. G. Ryskin, Eur. Phys. J. C **14**, 525 (2000) [arXiv:hep-ph/0002072].

- [11] M. G. Albrow and A. Rostovtsev, arXiv:hep-ph/0009336.
- [12] V. A. Khoze, A. D. Martin and M. G. Ryskin, Eur. Phys. J. C **23**, 311 (2002) [arXiv:hep-ph/0111078].
- [13] A. De Roeck, V. A. Khoze, A. D. Martin, R. Orava and M. G. Ryskin, Eur. Phys. J. C **25**, 391 (2002) [arXiv:hep-ph/0207042].
- [14] For a recent review see A. D. Martin, M. G. Ryskin and V. A. Khoze, arXiv:0903.2980 [hep-ph].
- [15] M. G. Albrow *et al.* [FP420 R&D Collaboration], arXiv:0806.0302 [hep-ex].
- [16] P. Bussey and P. Van Mechelen in: H. Jung *et al.*, arXiv:0903.3861 [hep-ph], p. 557.
- [17] C. Royon, Acta Phys. Polon. B **39**, 2339 (2008) [arXiv:0805.0261 [hep-ph]].
- [18] T. Aaltonen *et al.* [CDF Collaboration], Phys. Rev. Lett. **99** (2007) 242002 [arXiv:0707.2374 [hep-ex]].
- [19] T. Aaltonen *et al.* [CDF Collaboration], Phys. Rev. D **77**, (2008) 052004 [arXiv:0712.0604 [hep-ex]].
- [20] T. Aaltonen *et al.* [CDF Collaboration], Phys. Rev. Lett. **102**, 242001 (2009) [arXiv:0902.1271 [hep-ex]].
- [21] M. Albrow, arXiv:0909.3471
- [22] Mike Albrow and Jim Pinfold, private communication.
- [23] V. A. Khoze, A. D. Martin, M. G. Ryskin and W. J. Stirling, Eur. Phys. J. C **38** (2005) 475 [arXiv:hep-ph/0409037].
- [24] J. Pumplin, Phys. Rev. **D47** (1993) 4820.
- [25] F. Yuan, Phys. Lett. B **510**, 155 (2001) [arXiv:hep-ph/0103213].
- [26] V. A. Petrov and R. A. Ryutin, JHEP **0408** (2004) 013 [arXiv:hep-ph/0403189];
V. A. Petrov, R. A. Ryutin, A. E. Sobol and J. P. Guillaud, JHEP **0506** (2005) 007 [arXiv:hep-ph/0409118].
- [27] A. Bzdak, Phys. Lett. B **619** (2005) 288 [arXiv:hep-ph/0506101].
- [28] M. Rangel, C. Royon, G. Alves, J. Barreto and R. B. Peschanski, Nucl. Phys. B **774**, 53 (2007) [arXiv:hep-ph/0612297].
- [29] R. S. Pasechnik, A. Szczurek and O. V. Teryaev, Phys. Lett. B **680** (2009) 62 [arXiv:0901.4187 [hep-ph]] and references therein.
- [30] G. T. Bodwin, E. Braaten and G. P. Lepage, Phys. Rev. D **51** (1995) 1125 [Erratum-ibid. D **55** (1997) 5853] [arXiv:hep-ph/9407339].
- [31] N. Brambilla, A. Pineda, J. Soto and A. Vairo, Rev. Mod. Phys. **77** (2005) 1423 [arXiv:hep-ph/0410047];
N. Brambilla and A. Vairo, Acta Phys. Polon. B **38**, 3429 (2007) [arXiv:0711.1328 [hep-ph]].
- [32] V. A. Khoze, A. D. Martin and M. G. Ryskin, Eur. Phys. J. C **18**, 167 (2000) [arXiv:hep-ph/0007359].

- [33] M. G. Ryskin, A. D. Martin and V. A. Khoze, Eur. Phys. J. C **54**, 199 (2008) [arXiv:0710.2494 [hep-ph]];
M. G. Ryskin, A. D. Martin and V. A. Khoze, Eur. Phys. J. C **60** (2009) 249 [arXiv:0812.2407 [hep-ph]].
- [34] V.A. Khoze, A.D. Martin and M.G. Ryskin, JHEP **0605**, 036 (2006) [arXiv:hep-ph/0602247].
- [35] M. G. Ryskin, A. D. Martin and V. A. Khoze, Eur. Phys. J. C **60** (2009) 265 [arXiv:0812.2413 [hep-ph]].
- [36] J. Bartels, S. Bondarenko, K. Kutak and L. Motyka, Phys. Rev. D **73** (2006) 093004 [arXiv:hep-ph/0601128].
- [37] C. Amsler *et al.* [Particle Data Group], Phys. Lett. B **667**, 1 (2008) and 2009 partial update for the 2010 edition.
- [38] L.D. Landau, Dokl. Akad. Nauk SSSR **60** (1948) 213;
C.N. Yang, Phys. Rev. **77** (1950) 242.
- [39] D. Barberis *et al.* [WA102 Collaboration], Phys. Lett. **B440** (1998) 225; *ibid.* **B422** (1998) 399;
A. Kirk *et al.* [WA102 Collaboration], arXiv:hep-ph/9810221.
- [40] V. A. Khoze, A. D. Martin and M. G. Ryskin, Eur. Phys. J. C **24**, 581 (2002) [arXiv:hep-ph/0203122].
- [41] S. Aid *et al.* [H1 Collaboration], Nucl. Phys. B **472** (1996) 3 [arXiv:hep-ex/9603005].
- [42] A. D. Martin and M. G. Ryskin, Phys. Rev. D **64**, 094017 (2001) [arXiv:hep-ph/0107149].
- [43] A. G. Shuvaev, K. J. Golec-Biernat, A. D. Martin and M. G. Ryskin, Phys. Rev. D **60**, 014015 (1999) [arXiv:hep-ph/9902410].
- [44] J. H. Kuhn, J. Kaplan and E. G. O. Safiani, Nucl. Phys. B **157**, 125 (1979).
- [45] R. Barbieri, R. Gatto and R. Kogerler, Bound Phys. Lett. B **60**, 183 (1976).
- [46] V. A. Novikov, L. B. Okun, M. A. Shifman, A. I. Vainshtein, M. B. Voloshin and V. I. Zakharov, Phys. Rept. **41**, 1 (1978).
- [47] F. E. Close, G. R. Farrar and Z. p. Li, Phys. Rev. D **55**, 5749 (1997) [arXiv:hep-ph/9610280].
- [48] R. Barbieri, M. Caffo, R. Gatto and E. Remiddi, Phys. Lett. B **95**, 93 (1980).
- [49] R. Alkofer and C. S. Fischer, Fizika B **13**, 65 (2004) [arXiv:hep-ph/0309089].
- [50] M. Gluck, E. Reya and A. Vogt, Z. Phys. C **67**, 433 (1995).
- [51] L. Frankfurt, C.E. Hyde, M. Strikman and C. Weiss, Phys. Rev. **D75**, 054009 (2007);
arXiv:0710.2942 [hep-ph];
M. Strikman and C. Weiss, arXiv:0812.1053 [hep-ph].
- [52] E. Gotsman, E. Levin, U. Maor and J. S. Miller, Eur. Phys. J. C **57**, 689 (2008) [arXiv:0805.2799 [hep-ph]].
- [53] H. A. Peng, Z. M. He and C. S. Ju, Phys. Lett. B **351**, 349 (1995).
- [54] E. Stein and A. Schafer, Phys. Lett. B **300**, 400 (1993).

- [55] T. Mori *et al.* [BELLE Collaboration], J. Phys. Soc. Jap. **76** (2007) 074102 [arXiv:0704.3538 [hep-ex]];
H. Nakazawa *et al.* [BELLE Collaboration], Phys. Lett. B **615** (2005) 39 [arXiv:hep-ex/0412058];
S. Uehara *et al.* [BELLE Collaboration], arXiv:0903.3697 [hep-ex].
- [56] V. A. Khoze, A. D. Martin, R. Orava and M. G. Ryskin, Eur. Phys. J. C **19**, 313 (2001) [arXiv:hep-ph/0010163].
- [57] L. A. Harland-Lang *et al.*, in preparation.
- [58] M. Albrow *et al.*, CERN-LHCC-2006-039, CERN-LHCC-G-124, CERN-CMS-NOTE-2007-002, Dec 2006;
G. Anelli *et al.* [TOTEM Collaboration], JINST **3** (2008) S08007.
- [59] M. Albrow *et al.* [USCMS Collaboration], arXiv:0811.0120 [hep-ex];
J. W. Lamsa and R. Orava, arXiv:0907.3847 [physics.acc-ph].
- [60] G. V. Pakhlova, arXiv:0810.4114 [hep-ex];
Phys. Atom. Nucl. **72** (2009) 482 [Yad. Fiz. **72** (2009) 518].